Biocatalysis and Agricultural Biotechnology 58 (2024) 103223

Contents lists available at ScienceDirect

Biocatalysis and Agricultural Biotechnology

journal homepage: www.elsevier.com/locate/bab

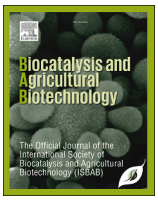

Nanoreinforcement strategies for enhancing biodegradable composites in biochemical applications within agriwaste valorisation

Imane Ziani [a, b, **], Abdelqader El Guerraf [b, c, d], Nour Eddine Bentouhami [e], Mohamed Brahmi [a], Hamza Bouakline [a], Ali El Bachiri [a], Marie-Laure Fauconnier [f], Sabah Ansar [g], Farooq Sher [h, *]

[a] Physical Chemistry of Natural Substances and Process Research Team, Laboratory of Applied Chemistry and Environment, Department of Chemistry, Faculty of Sciences, Mohammed First University, Oujda, 60000, Morocco
[b] International Society of Engineering Science and Technology, Nottingham, United Kingdom
[c] J. Heyrovsky Institute of Physical Chemistry, Dolejškova 2155, Libeň, 18200, Praha 8, Czech Republic
[d] Laboratory of Applied Chemistry and Environment, Faculty of Science and Techniques, University Hassan First, BP. 577, Settat, 26000, Morocco
[e] Laboratory of Bioresources, Biotechnology, Ethno-Pharmacology and Health, Department of Biology, Faculty of Sciences, Mohammed First University, Oujda 60000, Morocco
[f] Laboratory of Chemistry of Natural Molecules, Gembloux Agro-Bio Tech, University of Liège, Liège, Belgium
[g] Department of Clinical Laboratory Sciences, College of Applied Medical Sciences, King Saud University, P.O. Box 10219, Riyadh, 11433, Saudi Arabia
[h] Department of Engineering, School of Science and Technology, Nottingham Trent University, Nottingham, NG11 8NS, United Kingdom

ARTICLE INFO

Handling Editor: Dr. Ching Hou

Keywords:
Rosmarinus tournefortii de Noé
Sustainability
Bioconversion
Bio-based materials
Nano reinforcement
Antioxidant
Environment

ABSTRACT

Exploring secondary outputs, specifically leftover materials from steam distillation of *Rosmarinus tournefortii* de Noé, as agents for reducing metals introduces a novel approach to eco-friendly nanomaterial production. This concept aligns with the creation of environmentally conscious nanoparticles, showcasing potential across various fields, notably biomedicine. By utilizing *R. tournefortii* de Noé, successful synthesis of silver nanoparticles (AgNPs) was achieved, yielding nanoscale variations influenced by plant's by-products. Beyond structural aspects, investigating biomedical applications, focusing on antioxidant and antimicrobial properties. Consistently observing ~94.9–97.3% scavenging inhibition in water residues at different concentrations and enhanced antimicrobial efficacy against Gram-negative and Gram-positive bacteria and *Rhodotorula glutinis* yeast due to these residues. Moreover, a thorough examination using density functional theory unveiled a robust interaction between silver clusters and specific biomolecules found within the residues, namely homoplantaginin, protocatechuic acid-glycoside, caffeic, and rosmarinic acids (ranging from 130.62 to 357.05 kcal/mol). These compounds notably enhance reducing efficacy of Ag + ions and contribute to the enduring stability of AgNPs (ζ values: −22.8 mV and −17.2 mV). Furthermore, the study recognizes challenges in finding alternative surface modification agents and explores intricate toxicity mechanisms of silver nanoparticles, emphasizing their interactions with inflammation. Introducing promising nanomedicine approaches involving rosmarinic acid nanoparticles for inflammatory bowel disease and rheuma-

* Corresponding author. Department of Engineering, School of Science and Technology, Nottingham Trent University, Nottingham NG11 8NS, United Kingdom.
** Corresponding author. Physical Chemistry of Natural Substances and Process Research Team, Laboratory of Applied Chemistry and Environment, Department of Chemistry, Faculty of Sciences, Mohammed First University, Oujda 60000, Morocco.
E-mail addresses: imane.ziani95@outlook.com (I. Ziani), Farooq.Sher@ntu.ac.uk (F. Sher).

https://doi.org/10.1016/j.bcab.2024.103223
Received 5 March 2024; Received in revised form 26 April 2024; Accepted 10 May 2024
Available online 11 May 2024

toid arthritis, highlighting the potential of rosemary by-products derived compounds in innovative therapeutic interventions for diverse inflammatory conditions.

1. Introduction

Nanotechnology stands as one of the most rapidly advancing domains in realm of science and technology on a global scale. In this vein, the fabrication of metal nanoparticles constitutes an actively investigated area within nanotechnology, exhibiting exponential advancements across biomedical applications, nutritional sciences, and energy applications (Mittal et al., 2013). The challenge of achieving a biogenetic synthesis of uniformly sized nanoparticles with distinct shapes remains at forefront of biomaterials science. This achievement has also rendered substantial advantages within the pharmaceutical sector, particularly in struggle against an array of bacterial and viral infections (Huh and Kwon, 2011). A broad spectrum of techniques encompassing physical, chemical, biological, and hybrid methodologies is currently employed to engineer nanoparticles of varying properties. Nonetheless, physical and chemical synthesis methods are frequently hindered by elevated production expenses, ecological pollution, and biological hazards (Bereza-Malcolm et al., 2015). Consequently, the biological approach emerges as an alternative to traditional chemical and physical methods, serving as an eco-friendly avenue for nanoparticle production. Moreover, this approach obviates the necessity for costly, perilous, and toxic substances (Naghdi et al., 2022).

Ongoing investigations into bio-production of non-metallic substances through botanical extracts have unveiled a fresh avenue, offering swift and benign techniques within redox reaction for creation of environmentally conscious nanoparticles. A multitude of scholars have documented the biogenic synthesis of metal nanoparticles via plant leaf extracts, spotlighting their potential uses. This propensity is ascribed to the presence of secondary metabolites, encompassing phenolic acids, flavonoids, alkaloids, and terpenoids, which primarily contribute to conversion of ions into substantial metal nanoparticles (Pisoschi et al., 2022). Several antecedent studies have underscored proficiency of biosynthesized nanoparticles in regulating oxidative stress, genotoxicity, and changes associated with apoptosis (Zhang et al., 2018). Furthermore, nanoparticles boast an extensive array of applications within the domains of agriculture and plant sciences. For instance, through utilization of bioprocessing technology, nanoparticles can transform agricultural and food residues into energy (Tariq et al., 2023) and valuable by-products (Usmani et al., 2022).

Moreover, researchers have extensively explored the utilization of lignocellulosic biomass for synthesizing metallic nanoparticles, elucidating its manifold applications and advantages. Chen et al. (2023) emphasize green synthesis methods using biomass components like cellulose, hemicellulose, and lignin, resulting in nanoparticles with unique properties applicable in catalysis, sensing, and biomedicine. For instance, cellulose-derived nanoparticles exhibit high catalytic activity, with conversion rates exceeding 90% in chemical reactions, while hemicellulose-derived ones demonstrate exceptional sensing capabilities, detecting pollutants at concentrations as low as 1 ppb (Chen et al., 2023). Lignin-derived nanoparticles show promising antimicrobial properties, with inhibition rates of up to 95% against bacteria, underscoring sustainability (Chen et al., 2023). Conversely, Sankaran et al. (2021) focus on enhancing bioenergy production through biomass-to-nanoparticle conversion. They highlight the use of magnetite nanoparticles (MNPs) alongside alkaline pretreatment on rice straw, resulting in a significant increase in biogas and methane yield by 100% and 129% respectively (Sankaran et al., 2021). Additionally, incorporating nanoparticles into acid-functionalized magnetic nanoparticles boosts sugar production by 46% (Sankaran et al., 2021). Both studies underscore value of biomass for nanoparticle synthesis, addressing various fields and offering sustainable solutions.

Despite the widespread use of plant extracts for nanoparticle synthesis, one of the most recent and promising methods, based on natural “bio-laboratory,” is the use of biodegradable wastes generated by agricultural and food industries. Moreover, these waste materials are abundant, cost-effective, and readily available, obviating the need for elaborate pre-processing procedures. Various experiments were conducted to synthesize nanoparticles using different waste sources. In this context, zinc oxide nanoparticles were produced employing waste from Phoenix dactylifera as a bio-reductant for efficient dye degradation and antibacterial effectiveness in wastewater treatment (Rambabu et al., 2021). PVP-coated silver nanoparticles (PVP-AgNPs) were employed in municipal solid waste composting (Gitipour et al., 2013). Additionally, Fenton process employed copper nanoparticles derived from printed circuit boards to degrade mining surfactant (Martins et al., 2021). Secondary metabolites are the main metal-reducing agents in the “green” synthesis of nanoparticles, are found naturally in waste from the essential oil industry. Raw materials with a low essential oil content generate a lot of waste. Although distilleries generally dispose of their residues, these common practices can disrupt ecological balance of the site and result in the loss of valuable biologically active substances present in the waste (Da Silva et al., 2016).

Amidst the diverse tapestry of rosemary species, *Rosmarinus officinalis* L. stands revered for its therapeutic prowess and generous yield of its essential oils. However, a notable void exists in expansive landscape an absence of comprehensive exploration into species *Rosmarinus tournefortii* de Noé. While *R. officinalis* L., has received considerable attention, intricacies of *Rosmarinus tournefortii* de Noé have been largely overlooked. This study aims to fill this void by uncovering untapped potential of *Rosmarinus tournefortii* de Noé, particularly in utilizing its waste by-products for nanoparticle synthesis. Specifically, focus is on utilizing water and solid by-products as reduction agents for Ag, Zn, and Cu metal ions. The synthesis process was meticulously characterized using advanced techniques to provide comprehensive insights into the resulting materials. Additionally, specialized analyses were conducted to evaluate efficacy of biomolecules within each by-product, with a comparative analysis between water and solid by-products to understand their roles in nanoparticle synthesis and their effectiveness as reduction agents.

Moreover, the study delves into potential biological applications of synthesized nanoparticles, particularly their antioxidant and antimicrobial properties, suggesting promising avenues in medicine and materials science. However, challenges and unexplored territories remain. The exploration of alternative complexation agents for nanoparticle surface modification is identified as a growing re-

search area to enhance nanoparticle stability and functionality. Additionally, the study underscores promising potential for multi-functional health applications. Overall, this study showcases the ability to repurpose industrial by-products for eco-friendly nanoparticle synthesis, showcasing accomplishments while highlighting avenues for future investigation. This multidisciplinary approach positions by-product-derived nanoparticle synthesis as a key player in sustainable nanotechnology and its myriad applications.

2. Materials and methods

2.1. Plant material extraction

The untamed *Rosmarinus tournefortii* de Noé plant's fresh leaves were harvested amidst its flowering phase on March 13, 2020, within Megrez forest region of eastern Morocco, located at coordinates 34° 43′ 52.6″ N 2° 04′ 21.5″ W (Ziani et al., 2023). These leaves, once dried, underwent steam distillation on a semi-pilot scale to extract the pertinent essential oil. The liquid residue produced during steam distillation was separated from the solid residue through filtration using a 90 mm Whatman (GF/A) filter and subsequently concentrated utilizing a rotary evaporator. In the case of solid residue, it was pulverized and air-dried over a period of approximately 15 days. Following this, the residue was subjected to de-ionized water extraction for an hour. The resultant extracts from two categories of rosemary by-products, namely liquid and solid residues, were securely stored in amber glass vials and maintained at a refrigerated temperature of 4 °C until subjected to analysis.

2.2. Biosynthesis of silver, zinc and copper nanoparticles

In the process of green synthesizing Ag, Zn, and Cu-NPs, well-established protocol by Raut et al. (2014) was adapted with minor adjustments. The initial step involved dissolving 2.5 g of liquid and solid residue extracts in 50 mL of de-ionized water to formulate aqueous extracts. Silver nitrate, zinc nitrate and copper nitrate served as precursor materials for Ag, Zn, and Cu nanoparticles. The prepared extract was then introduced to 0.1 M solutions of $AgNO_3$, $ZnNO_3$, and $CuNO_3$, maintaining a ratio of 1:2 (v/v). The solution mixture was agitated at 70 °C for 3 h. After nanoparticle synthesis was finalized, centrifugation was employed to isolate Ag, Zn, and Cu-NPs. The supernatant was separated post-centrifugation, and resulting precipitates underwent triple washing using de-ionized water, followed by drying at 60 °C for two days (Fig. 1).

2.3. Characterization of biosynthesized nanoparticles

To confirm the generation of nanoparticles, a Shimadzu UV 1650-PC UV–visible spectrophotometer was utilized. The measurement of absorbance was carried out within the range of 300–800 nm (Lv et al., 2021). Attenuated Total Reflectance-Fourier Transform Infrared (ATR-FTIR) analysis was executed employing a Jasco 4700-FTIR spectrometer from Shimadzu, Japan. This was done to compare the characteristics of dried plant material with those of synthesized nanoparticles, aiming to decipher role of reducing agents in metallic ion reduction. The absorption spectra were captured over a wavelength range of 400–4000 cm^{-1} (Borah et al., 2021). Microstructural scrutiny of developed charged nanoparticles was performed using a JEOL-JSM7001F instrument and field-emission scanning electron microscopy (FE-SEM). SEM filament operated at various currents and a voltage of 5 kV at different magnifications, while fixed working distance was maintained at 6 mm (representing unchanging separation between sample and objective lens). Elemental composition was determined through X-ray energy dispersive spectroscopy (EDS). The mean diameter and distribution of the nanoparticles were measured using a laser granulometer, specifically Anton Paar Litesizer 500 (de Souza Niero et al., 2023). These measurements were executed at room temperature within a liquid cell containing a dispersant with a refractive index of 1.33. Zeta potential was determined via electrophoresis and application of Smoluchowski equation to analyze particle mobility. XRD patterns of all nanoparticle samples were captured using a Shimadzu XRD-6000 diffractometer and a Cu K (λ = 0.154 nm) radiation source. Data collection occurred at a scanning speed of 0.02°/s within a diffraction angle span of 10°–80°. The crystallite sizes of nanoparticles

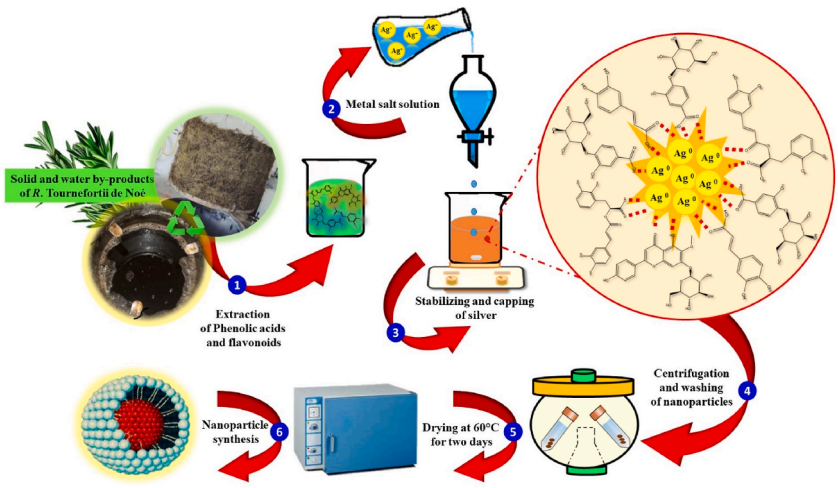

Fig. 1. The elaboration process of silver nanoparticles using *Rosmarinus tournefortii* de Noé by-products.

were deduced utilizing Scherrer formula (Eq. (1)) (El Guerraf et al., 2023), with average diameter of silver crystals (D) being calculated based on (111) plane.

$$D = \frac{K\lambda}{\beta\ COS\ \Theta} \tag{1}$$

2.4. Matrix of rosemary by-products

In the evaluation of rosemary by-products, a High-Performance Liquid Chromatography (HPLC) System, furnished with a 2998 Photodiode Array Detector and a reversed-phase C18 column (5, 250 × 4.6 mm), was utilized. Following the procedure outlined by Liu et al. (2011), extracts with a concentration of 5 mg/mL were introduced into column, flowing at a rate of 0.8 mL/min, utilizing a gradient mixture of binary solvents. To separate phenolic compounds, a mobile phase consisting of two constituents was employed: mobile phase A (acetonitrile with 0.1% formic acid) and mobile phase B (water with 0.1% formic acid). The gradient pattern followed this sequence: starting at 60% B at 0 min, transitioning to 50% B at 2 min, maintaining 50% B at 10 min, decreasing to 30% B at 15 min, maintaining 30% B at 25 min, and returning to 60% B at 35 min. To identify specific phenolic components, their retention time and maximum wavelength were assessed and compared against established standards and available literature data.

2.5. DPPH radical scavenging assay

The 2,2-diphenyl-1-picrylhydrazyl (DPPH) assay was carried out with a slight alteration derived from our previously outlined procedure (El Guerraf et al., 2023). This assay is commonly employed to evaluate the antioxidant potential of environmentally produced nanoparticles. In a concise summary, varying concentrations (0.1, 0.5, 1, 1.5 and 2 mg/mL) of the nanoparticles were mixed with 2500 μL of DPPH solution in methanol (0.04 mg/mL). After being left in the dark for 60 min, the absorbance at 517 nm was gauged via a UV–vis spectrophotometer. The scavenging inhibition (%) was determined using the subsequent formula, depicted by **Eq. (2)**, in which A0 symbolizes the absorbance of the control, and AC signifies the absorbance of the tested samples.

$$DPPH\ Inhibition\ (\%) = \frac{A0 - AC}{A0} \times 100 \tag{2}$$

2.6. Anti-microbial properties

Following prior investigations (Abdollahzadeh et al., 2021), agar diffusion method was employed to assess antibacterial properties of nanoparticles synthesized from rosemary by-products on solid surfaces. The in vitro antibacterial performance was evaluated against distinct microorganisms, namely *Staphylococcus aureus* (gram-positive bacteria), *Escherichia coli* ATCC 25922 (gram-negative bacteria), along with *Rhodotorula glutinis* (yeast) and *Geotrichum* sp. (mould). For both microbial types, strains were adjusted to a 0.5 McFarland standard, equivalent to 10^6 CFU/mL and 10^6 spores/mL, correspondingly (Mahdi et al., 2022). Afterwards, these cultures were additionally thinned using Mueller-Hinton broth for bacteria, yeast, and mould, and sterile physiological water for both, before being introduced onto the surface of petri dishes. In this approach, wells (6 mm) were generated in Mueller-Hinton agar (MHA) previously inoculated with the target bacteria or fungus. These wells were subsequently loaded with 10 μL of samples (10 mg/mL). Incubation of agar plates facilitated bacterial and fungal growth, conducted at 37 °C for 18 h and 25 °C for 48 h, respectively. The antimicrobial efficacy was evaluated by measuring size of the inhibition zone within agar medium. To ensure robustness, each assay was carried out in triplicate.

2.7. Computational study

Initially, major compounds (caffeic acid, homoplantaginin, protocatechuic acid-glycoside, rosmarinic acid, epicatechin and gallocatechin) extracted from *Rosmarinus tournefortii* de Noé by-products were optimized at the ground state using GAUSSIAN 09 quantum chemistry simulation software (Kaushik et al., 2022). Subsequently, each individual molecule was optimized in conjunction with a silver cluster by placing it in close proximity to reactive sites that were identified through analyses of molecular electrostatic potential (MEP). To reduce computational costs, representative models of silver nanoparticles (AgNPs), consisting of a single silver atom (Ag_1) and three silver atoms (Ag_3) clusters, were utilized. The interaction energies between AgNPs models and target molecules were estimated using **Eq. (3)** (Kaushik et al., 2022).

$$\Delta I = E_{Ag\text{-}compound} - \left(E_{Ag} + E_{compound}\right) \tag{3}$$

Where $E_{Ag\text{-}compound}$, E_{Ag} and $E_{compound}$ represent energies associated with interaction between AgNPs and target molecule, AgNPs themselves and the target compound, respectively. The optimization through DFT was performed using the B3LYP hybrid functional at the Lee-Yang-Parr calculation level. The organic compounds underwent treatment with 6-311G(d,p) basis set, whereas Ag atoms were characterized using the LanL2DZ basis set. Conventional convergence criteria were applied and visualization of molecular structure was facilitated using GaussView 5.0 molecular editor.

3. Results and discussion

3.1. Optical absorption and crystalline structure analysis

UV–vis spectroscopy is a highly effective method for analyzing optical response of metal nanoparticles, particularly sensitive to their formation due to pronounced surface plasmon resonances (SPRs) they exhibit (Kelly et al., 2003). In this study, the UV–vis ab-

sorption spectra of colloidal nanoparticles produced from two types of rosemary residues were examined. The spectral data demonstrated distinctive surface plasmon (SP) bands associated with AgNPs, showing variations in their "λ_{max}" and intensity of SP band. This distinction underscores the evident impact of compound's characteristics on these particular parameters. In contrast, when Zn and Cu were employed for nanoparticle synthesis, SP band intensity spectra remained unchanged, indicating unsuccessful development of ZnNPs and CuNPs. The consistent surface plasmon (SP) band intensity spectra observed during the utilization of Zn and Cu for nanoparticle synthesis suggest unsuccessful development of ZnNPs and CuNPs, potentially due to various factors. Inadequate synthesis conditions, such as suboptimal temperature, pH, or reaction time, could have led to formation of nanoparticles with properties deviating from the desired plasmonic characteristics (Kim et al., 2024).

Additionally, propensity of Zn and Cu nanoparticles to oxidize in air or aqueous environments may have resulted in the formation of oxide layers on nanoparticle surface, affecting their plasmonic properties (Jahan et al., 2021). Agglomeration or aggregation of nanoparticles during synthesis or post-synthesis treatments could have altered the interactions between nanoparticles, impacting observed SP band intensities (Pryshchepa et al., 2020). Furthermore, surface contamination with impurities or residues from the synthesis process might have interfered with plasmonic properties of ZnNPs and CuNPs. The absence of appropriate surface ligands or stabilizing agents during synthesis could have led to unstable nanoparticles with modified plasmonic behavior (Kim et al., 2023). These factors collectively contribute to challenges in achieving successful development of ZnNPs and CuNPs with the desired plasmonic properties.

The spectra were captured when colloidal sample's colour and absorption strength remained constant. Fig. 2**(a)** and **(b)** illustrates that each residue used exhibits a single, distinct SPR position in 300–500 nm range. Additionally, no SPRs were seen at wavelengths greater than 500 nm, suggesting that the majority of AgNPs produced have small sizes and comparable shapes. This observation also provides early clues about colloidal AgNPs' size and size distribution. Comparing plasmon band positions of two different residues, solid residue revealed higher wavelengths (372 nm) than water residue (368 nm), demonstrating a reduction in AgNPs particle size.

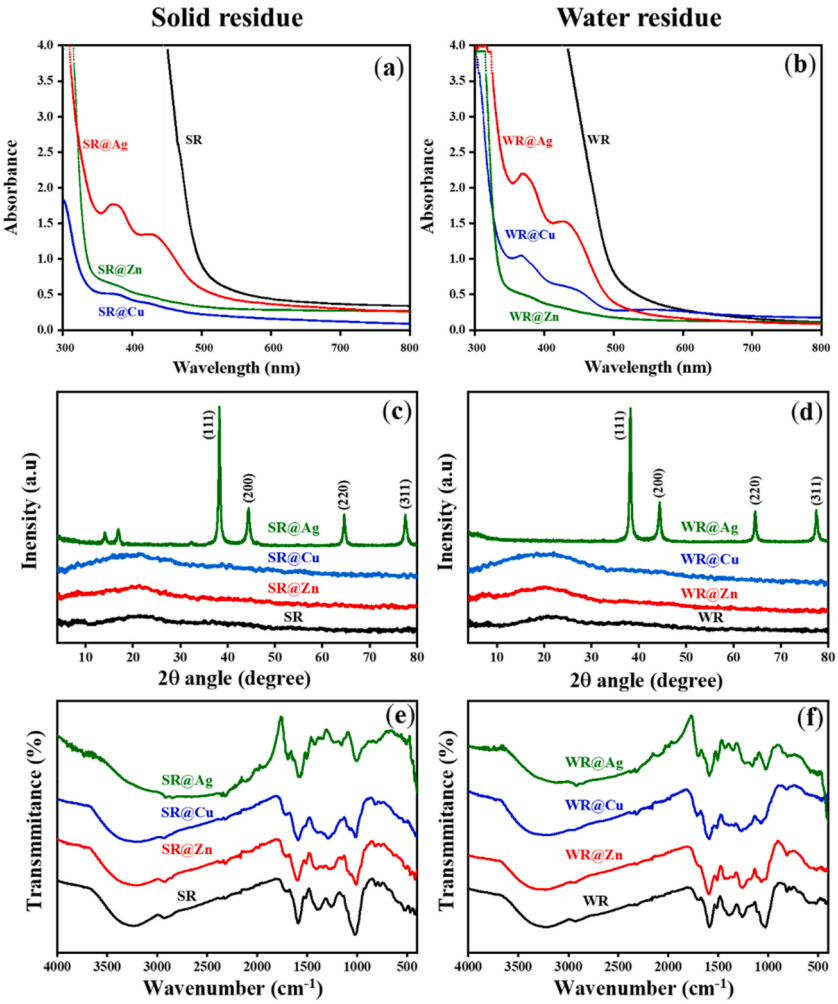

Fig. 2. (a, b) UV–visible patterns, (c, d) X-ray diffraction patterns and (e, f) FTIR profiles of biosynthesized nanoparticles using *Rosmarinus tournefortii* de Noé solid and water residues.

Similar to this, several earlier studies from *Rosmarinus officinalis* L. plant species have also noted absorption spectrum between 350 and 500 nm brought on by AgNPs' surface plasmon resonance (Ghaedi et al., 2015; Noukelag et al., 2021).

X-ray diffraction (XRD) and Fourier-transform infrared spectroscopy (FTIR) were conducted to gain information on the one hand about size, lattice and structure of nanoparticles and on the other hand, about any potential bioactive compounds present in *Rosmarinus tournefortii* de Noé and that can possibly act as reducing/stabilizing agent. For a better comparison, the spectroscopic analysis was achieved in case of Zn, Cu and Ag biosynthesized in the presence of two types of rosemary by-products; solid and water residues. Firstly, by analysing XRD pattern obtained for the tested by-products, it is clear amorphous nature of both SR and WR (Fig. 2**(c)** and **(d)**). When using Zn or Cu, the XRD spectra remain unchanged suggesting unsuccessful elaboration of ZnNPs and CuNPs. The diffractograms resulted for silver nanoparticles were totally different as they showed four well-resolved peaks at 2θ angles of 38.27°, 44.38°, 64.62° and 77.52° for SR, and 38.15°, 44.32°, 64.55°, and 77.45° in the case of WR. These prominent peaks arise from (111), (200), (220) and (311) Bragg reflections of face-centred cubic (fcc) structures of AgNPs (JCPDS 04–0783). Further, the average crystallite size (d) of AgNPs was estimated using Debye-Scherrer equation, $d = K\lambda/\beta\cos\theta$ where K is the shape factor (between 0.9 and 1.1), λ is the incident X-ray wavelength of Cu Kα radiation (1.542 Å), β is the full width at half maximum in radians of (111) line and θ is the Bragg diffraction angle. The average AgNPs sizes were found to be 17.98 and 18.49 nm for SR@AgNPs and WR@AgNPs composites, respectively. The obtained results are more interesting than those of Das et al. (Das and Velusamy, 2013) and Ghaedi et al. (2015) where it was reported that the mean AgNPs particle size ranged from 31.79 to 33 nm for the plant genus *Rosmarinus officinalis* L. respectively.

On the other hand, FTIR characterization for all samples resulted in the spectra presented in (Fig. 2**(e)** and **(f)**). For both SR and WR, several typical bands were observed that describe functional groups associated with various biological macromolecules in Rosemary leaf extracts. The peak with relatively high intensity at 1020 cm^{-1} is assigned to C–O–C stretching vibration or alcohols/phenols (Farshchi et al., 2018). The bands at around 1152 and 1256 cm^{-1} arise from C–O stretching and represent the presence of polyphenols and one that appears at 1391 cm^{-1} corresponds to C–O–C stretching modes of vibration. The signal at 1514 cm^{-1} demonstrates also the presence of phenolic compounds from extract which is related to stretching of the aromatic rings (Farshchi et al., 2018). The peak detected at approximately 1587 cm^{-1} may result from vibration of C=C groups, while the one near 1713 cm^{-1} is associated with C=O groups from carboxylic acids (Piñeros-Hernandez et al., 2017). The stretching vibration of C–H is justified by the peak appearing at 2931 cm^{-1}. Finally, the broad absorption band at a wavenumber between 3020 and 3620 cm^{-1} is linked to O–H stretching (Piñeros-Hernandez et al., 2017).

After the bio-synthesis of AgNPs, spectrum remains practically unchanged demonstrating that metal nanoparticles did not alter structure of the rosemary plant in a significant way. It should be noted, however, that some IR bands were shifted to lower frequencies after the interaction of residues with Ag. Based on ATR-FTIR results and previously reported papers for *Rosmarinus officinalis* L. species (Rabiee et al., 2020), mechanism of reducing silver ions to metallic silver can be discussed. In a simple way, numerous bioactive compounds from *Rosmarinus tournefortii* de Noé will surround Ag^{+} producing a coating. The latter receive electrons from these phytochemical constituents resulting in the reduction of silver cation and avoiding agglomeration of particles. Most likely, the carbonyl groups from bioactive compounds are responsible for the reduction process and can act as a stabilizer and bio-capping agents of the AgNPs. In summary, spectroscopic analyses have demonstrated the successful green synthesis of AgNPs using both *Rosmarinus tournefortii* de Noé solid and water residues. Apart from Zn and Cu, no promising results were obtained, which may be related to the absence of sufficient reducing agents or suitable biomolecules to facilitate the reduction of metal ions, thus hindering NPs formation.

The limitations in ATR-FTIR analysis, despite comparing plant extract with synthesized CuNPs or ZnNPs, stem from challenges inherent in nanoparticle synthesis process, as evidenced by prior UV–vis and DRX analyses. Incomplete reduction of metal ions during synthesis may hinder the formation of well-defined nanoparticles with distinct chemical characteristics (Adra et al., 2024). Moreover, issues like nanoparticle aggregation or precipitation, due to inadequate stabilization or unfavorable reaction conditions, can obscure changes in ATR-FTIR spectra. These aggregated nanoparticles may exhibit broad or overlapping peaks, making it challenging to discern specific features. Additionally, the sensitivity of ATR-FTIR may not be sufficient to detect subtle changes in chemical composition or surface functional groups, particularly with low nanoparticle concentration or minimal changes (Lee and Chae, 2021). Background signals or noise in the spectra could further complicate analysis. Weak or transient interactions between plant extract components and Cu or Zn ions may result in subtle or undetectable changes in FTIR spectra, possibly due to the nature of binding sites on plant's extract molecules (Jędrzejczyk et al., 2023). Together, these factors contribute to the limited changes observed in ATR-FTIR analysis following unsuccessful nanoparticle synthesis. As the mechanism of interaction remains always hard to fully understand, further optimization of experimental conditions may be necessary in future studies. It is essential to highlight that this study primarily concentrated on the synthesis of nanoparticles from *Rosmarinus tournefortii* de Noé, a species not previously investigated for this purpose, suggesting avenues for future exploration.

3.2. Hydrodynamic size and surface analysis

The enduring stability of colloidal silver nanoparticles was observed through spectroscopic monitoring using zeta potential technique. This method, commonly employed for managing stability of colloidal metal nanoparticles, gauges alterations in surface charge. Metal nanoparticles possessing a notably positive or negative zeta potential exhibit mutual repulsion, preventing them from aggregating. Conversely, particles with low absolute zeta potential values tend to aggregate and coalesce due to the absence of repulsive forces that hinder such accumulation (Rao et al., 2021). Zeta potential (ζ) results for two types of *Rosmarinus tournefortii* de Noé steam distillation by-products; solid residues and water have ζ values of −13.3 and −11.4 mV, while freshly prepared colloidal AgNPs have ζ values of −22.8 and −17.2 mV, respectively. The results obtained showed a strong negative value for AgNPs, clearly suggesting stability of nanoparticles. Moreover, the stability and colloidal behaviour of nanoparticles were explored as shown in Fig. 3**(a)** and

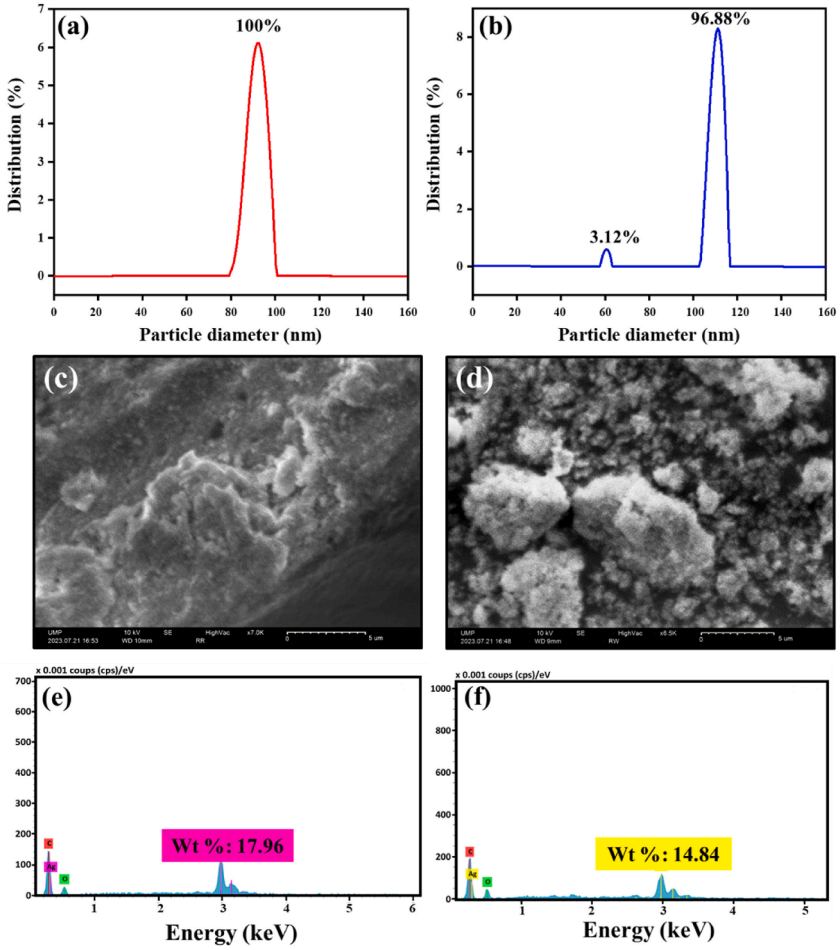

Fig. 3. Hydrodynamic size**,** SEM images and corresponding EDS spectra of synthesized AgNPs using *Rosmarinus tournefortii* de Noé; (a, c, e) solid and (b, d, f) water residues.

(b), yielding insightful findings. Notably, a single peak position was observed on the distribution graph for SR@AgNPs, indicating that nanoparticles in this residue exhibited a uniform size of approximately 92.3 nm and shared a similar surface charge. Such uniformity is characteristic of a monodisperse (narrowly distributed) sample, which holds significant appeal for numerous applications. Additionally, intriguingly, WR@AgNPs displayed two distinct peaks in nanoparticle size distribution (62.2 and 111.64 nm). Each peak represented a group of particles with comparable sizes. This bimodal distribution suggested existence of two separate populations of nanoparticles in the sample. Possible explanations for this phenomenon could include aggregation or agglomeration of nanoparticles, resulting in larger particles that contribute to the second peak in size distribution. Furthermore, the presence of various morphologies or crystalline structures among the nanoparticles might also contribute to bimodal size distribution. For instance, certain metal nanoparticles can exhibit different shapes, such as spherical and rod-shaped, leading to diverse size populations (Yaraki et al., 2022).

Additional support for the successful production of AgNPs was uncovered through morphological examinations and elemental analysis. As illustrated in Fig. 3**(c)** and **(d)**, the obtained nanoparticles exhibited distinct shapes. The two types of by-products displayed predominantly spherical morphology in their nanoparticles, each exhibiting varying diameters within the nanoscale range. Because of their diminutive size, extensive surface activity and considerable specific surface area, the nanoparticles had a proclivity to readily form aggregates. The effectiveness of synthesizing AgNPs using *Rosmarinus tournefortii* de Noé solid and water residues was further confirmed by analyzing chemical composition based on EDX spectrum (Fig. 3**(e)** and **(f)**). The optical absorption band of the EDX peak in3–4 keV range is characteristic of metallic silver nanocrystallites' absorption (Kotakadi et al., 2014). The EDX spectrum of the synthesized silver nanoparticles (Fig. 3**(e)** and **(f)**) clearly showed absence of elemental nitrogen peaks and the presence of elemental silver metal, along with C and O, which are associated with phenolic compounds of residues and formation of Ag NPs. The distinct signal peak of silver provided strong evidence of the successful reduction of silver nitrate to silver nanoparticles. Our findings align with earlier studies on AgNPs produced from *Rosmarinus officinalis* L. plant species (Das and Velusamy, 2013; Ghaedi et al., 2015). Those studies also noted the presence of uniformly sized, spherical silver nanoparticles in nanoscale range.

3.3. Matrix responsible for metal ion reduction

Many active plant chemicals with therapeutic or dietary benefits have been used to create nanomaterials. Among these, flavonoids and phenolic acids have received a great deal of attention because of their potential uses in nano-medicine. To better understand the nature of the molecules responsible for stabilization and reduction in synthesis of metal NPs, HPLC-DAD analysis was carried out. Through comparing retention times and UV–visible spectra of specimens with established reference standards, it was possible to swiftly identify the presence of gallic acid, epicatechin, chlorogenic acid, rosmarinic acid, caffeic acid and apigenin. To identify the flavonoids, data relating to flavonoid elution scheme as described in the literature were also examined in detail. Both types of rosemary steam distillation by-product extracts contained phenolic acids and flavonoids, which have been tentatively identified in Table 1 as two families.

According to reference standards, peak 1,2, 3/6, 7/5, 9/7 and 10/8 for solid and water (SR/WR) residues, respectively, were positively identified as chemical structures of gallic acid, epicatechin, chlorogenic acid, caffeic acid, rosmarinic acid and apigenin (Fig. 4). The same identification was discovered by prior studies for rosemary (Bendif et al., 2017). Additionally, since the third peak's absorbance band falls within 275–340 nm range, values that are nearly identical to UV–vis spectra detected by numerous studies (270–340 nm), the third peak may be assumed to be homoplantaginin for solid residue extract (Miguel Herrero et al., 2010). According to UV–vis spectrum of peak 4 for water residue, protocatechic acid glycoside was recognized for this peak with maxima at 220.0 and 281.2 nm, which is almost identical to the spectra given by literature data for the same plant (M. Herrero et al., 2010). For peaks 4 and 5 for solid and water residues, respectively, flavanol gallocatechin is highly recommended, whose maximum spectra were recorded between 283 and 335 nm, values quite close to those corresponding in present study (283, 334 nm). Further, the patterns of two UV spectra are similar, demonstrating that those peaks are linked to gallocatechin (Almela et al., 2006). Based on the spectrum maximum at 275.3 nm, which is characteristic of spectral maxima observed in several studies (de Almeida Gonçalves et al., 2018; Gonçalves et al., 2019), yunnaneic acid F is the most suggested structure for peak 8 of water residue extract.

Table 1
Identification of phenolic compounds from *Rosmarinus tournefortii* de Noé responsible for metal ion reduction.

Peak number	Retention time (min)		Tentative identified compounds		Relative abundance (% of total peak area)	
	Water residue	Solid residue	Water residue	Solid residue	Solid residue	Water residue
1	2.13	3.41	Gallic acid	Gallic acid	9.65	0.92
2	2.66	3.92	Epicatechin	Epicatechin	17.22	7.82
3	3.03	4.39	Chlorogenic acid	Homoplantaginin	15.52	4.94
4	3.27	5.63	Protocatechuic acid- glycoside	Gallocatechin	12.24	32.05
5	3.66	5.80	Gallocatechin	Caffeic acid	31.02	4.25
6	3.99	7.84	N. I	Chlorogenic acid	2.56	2.79
7	4.43	7.95	Caffeic acid	Rosmarinic acid	3.81	23.51
8	6.08	8.80	Yunnaneic acid F	Apigenin	1.68	1.33
9	6.52	–	Rosmarinic acid	–	–	21.15
10	9.32	–	Apigenin	–	–	1.21

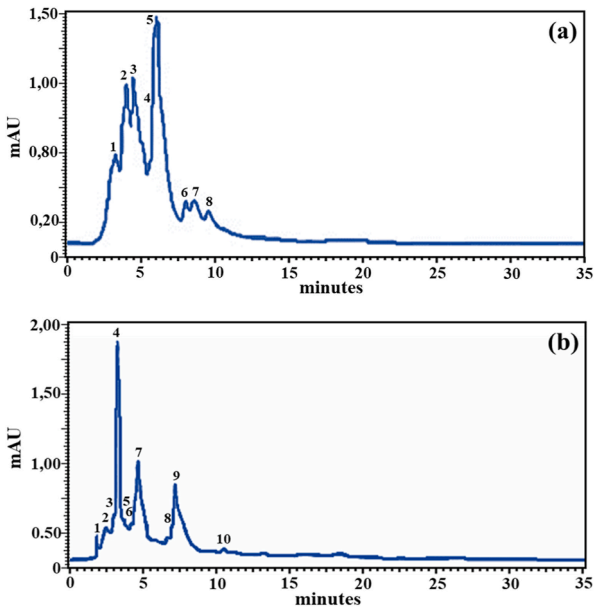

Fig. 4. HPLC-DAD chromatograms of; (a) Solid and (b) Liquid by-products of *Rosmarinus tournefortii* de Noé.

Comparing two aqueous by-product extracts, water residue remained to extract more phenolic compounds than the solid residue that could be attributed to prolonged contact of the plant material with boiling water, a cell permeation effect favoring the extraction of metabolites can be assumed. The harsh steam distillation conditions can also cause the formation of phenolic artefacts in water residue. In addition, high recovery of rosmarinic acid and protocatechuic acid glycoside was revealed in water residue, while epicatechin and homoplantagenin had to be extracted to maximum in the solid residue. Caffeic acid is extracted in almost the same way in both residues, meaning that it takes longer to extract it in its entirety in aqueous residue. These findings align with prior observations by Miljanovic' et al. (Miljanović et al., 2023), indicating a higher efficacity of phenolic acid (rosmarinic, syringic and caffeic acids) and flavonoid (gallocatechin and apeginin) extraction in both by-products, especially in water residue. However, a limitation arises from inability to compare products using ethanol/water as the extraction solvent for solid residue, hindering a comprehensive analysis. Discrepancies with the findings of Luca et al. (2023), highlight that solid and water residues had the same elution pattern for most polar compounds, while phenolic diterpenes were absent in the water residue. The authors compared two by-products with a different solvent extract, for which the solid residue was extracted using SC-CO_2 extraction or even solid residue from hydrodistillation extracted with methanol/water, which is normal to have phenolic diterpenes since solvents used can rapidly extract a range of molecule polarities.

Moreover, observations from Wollinger et al. (2016) regarding limited phenolic compound presence in water residue (rosmarinic acid and traces of carnosol and carnosic acid) underscore the potential impact of distillation process duration. Conversely, studies by Celano et al. (2017) and de Elguea-Culebras et al. (de Elguea-Culebras et al., 2023) reported the presence of all phenolic compounds, including phenolic diterpenes, in water residue, emphasizing the complexity of compound extraction influenced by solvent choice and extraction method. Despite these insights, a comprehensive elucidation of the comparison between two aqueous extracts from steam distillation by-products remains elusive, warranting further investigation. Limited published data on the chemical composition of aqueous residue from rosemary distillation, particularly for *Rosmarinus officinalis* L. and *Rosmarinus tournefortii* de Noé species, underscores the need for future research to validate these findings.

3.4. DPPH radical scavenging by elaborated nanoparticles

Antioxidants are widely acknowledged for their potential efficacy in treating and preventing various diseases. However, a notable limitation arises from low permeability and poor water solubility of most antioxidants, leading to instability during storage and degradation in gastrointestinal tract (Oliveira et al., 2021). Consequently, their practical utility has been restricted. To address this issue, the amalgamation of materials science and nanotechnology has played a pivotal role in reducing the generation of free radicals during nanoparticle production. These specialized nanoparticles, termed nano-antioxidants, have emerged as a solution (Dal Lago et al., 2011). In this study, nanoparticles' capacity to mitigate DPPH free radical was investigated. The efficacy of prepared samples in this regard was assessed using a straightforward methodology, measuring their scavenging activity against this stable free radical.

Antioxidant capacities of elaborated materials are presented in Fig. 5. For comparison, two types of *Rosmarinus tournefortii* de Noé by-products were also tested and results are illustrated in the same figure. Ashighlighted, arrangement of two types of by-products is the same, for which incorporated AgNPs showed significantly higher inhibition in the case of SR/WR@AgNPs than the free by-products extracts, while unsuccessful SR/WR@CuNPs and SR/WR@ZnNPs syntheses showed lowest entrapment with DPPH inhibition respectively. Furthermore, upon comparing evaluated scavenging capacities of two by-product types, water residue emerged as the most effective for incorporation. Notably, scavenging inhibition, ranging from 94.9 to 97.3%, remained consistently stable across tested concentrations. Conversely, solid residue exhibited an escalating inhibition with increasing concentrations (ranging from 68.11 to 97.2%), as depicted in Fig. 5. Considering these compelling results, observed differences in composition could indeed be attributed to distinct chemical structures present in each by-product. In this context, chemical profile obtained through HPLC-DAD analysis revealed a delicate equilibrium between flavonoids (46.34%) and phenolic acids (37.39%) in solid residue. On the contrary, in liquid residue, a striking predominance of phenolic acids (50.9% hydroxycinnamic acids and 32.97% hydroxybenzoic acids) over flavonoids (13.28%) was observed, leading to intriguing possibilities.

Comparing two types of phenolic acids and flavonoids, Bhutto et al. (2018) explored correlation between antioxidative potential of phenolic compounds and plasmon characteristics of silver nanoparticles. The study revealed that flavonoids exhibit a strong optical

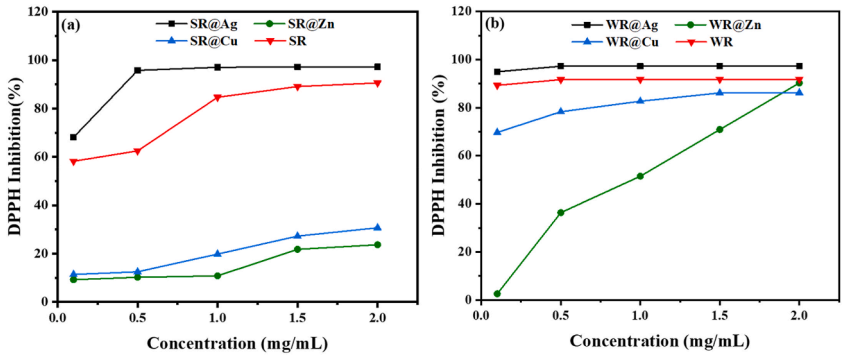

Fig. 5. Antioxidant performance of (a) Solid and (b) Water by-products and their coating with Ag, Cu and Zn.

response facilitated by developed AgNPs, contrasting with phenolic acids. Within phenolic acids, hydroxycinnamic acid generally outperformed hydroxybenzoic acids, as assessed through both UV–vis bands and the corresponding molar absorptivity for these two types of phenolic acids. The same trend was found in the study performed by Scroccarello et al. (2021), where it was reported that AgNPs formed with relative caffeic acid were significantly higher than gallic acid as one of the most hydroxybenzoic acids used. The nucleophilicity of corresponding structures that react in an alkaline medium was likely responsible for difference in optical responses of AgNPs prepared by hydroxybenzoic and hydroxycinamic acids. The nucleophilicity of phenolics is affected by the substitution of electron-donating (-OH and OCH_3) and electron-withdrawing (-COOH and –CH = CH–COOH) groups and this has an impact on how AgNPs respond optically.

Based on these compelling data, the highest activity of WR@AgNPs can be attributed to remarkable influence of phenolic acids, particularly rosmarinic and caffeic acids. Their exceptional ability to swiftly and effectively neutralize free radicals significantly enhances antioxidant properties of nanoparticles, surpassing the collective effect of combining flavonoids and phenolic acids. These rapid and potent free radical scavenging capabilities play a pivotal role in bolstering the antioxidant efficacy of WR@AgNPs. The pivotal role of phenolic acids, particularly rosmarinic and caffeic acids, in driving nanoparticles' robust antioxidant prowess is paramount in battle against oxidative stress (Mohamad Sukri et al., 2023). The intricate interplay between these phenolic compounds and nanoparticle matrix results in potent antioxidant effects, as evidenced by remarkable 95% scavenging potential against free radicals showcased in the study of Harsha Haridas et al. (Harsha Haridas et al., 2023). Caffeic acid's renowned antioxidant properties are central to neutralizing reactive oxygen species and preventing oxidative damage within biological systems, facilitated by its controlled release encapsulated within the nanoparticles. Moreover, in model physiological media, rosmarinic acid demonstrated robust radical scavenging activity with overall rate constant values of 2.89×10^{10} and 3.86×10^{9} M^{-1} s^{-1} in water and pentyl ethanoate solvents, respectively (Vo et al., 2023). Furthermore, in an aqueous environment, rosmarinic acid exhibited an overall rate constant of 3.18×10^{8} M^{-1} s^{-1} for scavenging $HOO^{\bullet}$, a value approximately 2446 times greater than Trolox, a common antioxidant compound (Vo et al., 2023).

These results highlight the potent antioxidant efficacy of rosmarinic acid, underscoring its pivotal role in enhancing antioxidant prowess of nanoparticles. The collaborative action between rosmarinic and caffeic acids and nanoparticles creates a synergistic effect, amplifying their combined antioxidant capabilities and underscoring their potential as effective therapeutic agents for combating oxidative damage and promoting cellular health. Through the donation of hydrogen atoms or electrons and chelation of transition metal ions, these nanoparticles derived from rosmarinic and caffeic acids exhibit exceptional antioxidant prowess crucial in mitigating oxidative stress and fostering overall cellular well-being (Bouammali et al., 2023). This dominance of phenolic acids highlights their pivotal role in driving the nanoparticles' robust antioxidant prowess, making them key players in the battle against oxidative stress (Vieira et al., 2022). Interestingly, synergy between flavonoids and phenolic acids does not consistently result in a proportional increase in antioxidant activity (Barbieri et al., 2020). In some instances, certain flavonoids may even interfere with antioxidant mechanisms of phenolic acids, leading to a potentially less effective overall antioxidant response.

3.5. Nanoparticles effect on microbial growth

Increased mortality, morbidity, and treatment costs in developing nations are thought to be primarily caused by MDR bacterial strains and infections they cause. Gram-positive, Gram-negative bacteria, moulds and yeast pathogens have all been linked to serious clinical and medical problems (Dakal et al., 2016). Thus, wide-ranging and potent volatile compounds present in rosemary essential oil allow it to effectively combat a broad spectrum of microorganisms, making it a valuable and promising natural substitute for phenolic compounds in combating infections and microbial growth. Additionally, nanoparticles can enhance antimicrobial efficacy of polar phenolic compounds, resulting in comparable or even superior effects to those of essential oils. In this proposal, agar diffusion test was used to assess antibacterial activity of the synthesized nanoparticles against two susceptible bacterial strains, *E. coli* and *S. aureus*, as well as yeast *Rhodotorula glutinis* and mould *Geotrichum* sp. Table 2 shows information regarding antimicrobial potential. Regarding two by-products of *R. Tourneforti* de Noé obtained through steam distillation and used as controls, the results revealed inhibition zones of 9.2 and 9 mm for *E. coli*, and 8.7 and 8.8 mm for *S. aureus*, in solid and water residues, respectively. For fungi, inhibition zones were measured at 10 and 9.8 mm for *Geotrichum* sp., and 14.3 and 15.2 mm for *Rhodotorula glutinis*, in solid and water residues, respectively.

Table 2
Inhibition Zones of the biosynthesized nanoparticles using *Rosmarinus tournefortii* de Noé solid and water residues.

Samples	Inhibition zone diameter (mm)			
	Escherichia coli	*Staphylococcus aureus*	*Geotrichum sp.*	*Rhodotorula glutinis*
WR	9 ± 0.78	8.8 ± 0.67	9.8 ± 0.53	15.2 ± 0.45
WR@ZnNPs	8.9 ± 0.35	8.7 ± 0.95	10 ± 0.33	16.1 ± 0.23
WR@CuNPs	9 ± 0.11	9.5 ± 0.22	9.6 ± 0.22	13 ± 0.25
WR@AgNPs	12 ± 0.49	13.8 ± 0.25	10 ± 0.63	16.8 ± 0.56
SR	9.2 ± 0.13	8.7 ± 0.46	10 ± 0.33	14.3 ± 0.13
SR@ZnNPs	9.6 ± 0.21	8.8 ± 0.47	9 ± 0.7	14.7 ± 0.31
SR@CuNPs	8.9 ± 0.22	9 ± 0.88	10.2 ± 0.22	15.2 ± 0.12
SR@AgNPs	13.2 ± 0.63	14 ± 0.98	9.8 ± 0.25	17.4 ± 1.02

As indicated in Table 2, unsuccessful biosynthesis SR/WR@ZnNPs and SR/WR@CuNPs had no effect and the antimicrobial activity did not change significantly for which diameter measurements of inhibition bacteria or fungi varied weakly indicating that phenolic compounds detected for two by-products of *R. Tourneforti* de Noé may not provide sufficient stabilization for NPs formed, leading to rapid agglomeration or degradation of NPs. Adequate stabilization is essential to prevent NPs from losing their antimicrobial efficacy. In contrast, the successfully biosynthesized nanoparticles, SR/WR@AgNPs, demonstrated a notable increase in inhibition zone against Gram-negative *E. coli* (12 and 13.2 mm for water and solid residues, respectively) and Gram-positive *S. aureus* (13.8 and 14 mm for water and solid residues, respectively). Similarly, the antimicrobial activity against yeast *Rhodotorula glutinis* was significantly enhanced (16.8 and 17.4 mm for solid and water residues). However, no significant change in antimicrobial activity was observed against mould *Geotrichum* sp. compared to two by-products without AgNPs. Furthermore, it was observed that two by-products, whether incorporated with Ag or not, exhibited higher activity against Gram-positive bacteria compared to Gram-negative bacteria. Comparing two nanoparticles, SR@AgNPs appear to be more active than WR@AgNPs against two Gram bacteria, while the opposite is true for yeast *Rhodotorula glutinis*.

Upon analyzing the results from each residue matrix, a compelling equilibrium between flavonoids and phenolic acids emerged in solid residue of *R. Tourneforti* de Noé. Intriguingly, over 80% of phenolic acids were concentrated in water residue, unveiling a distinct distribution pattern between these two compound types within the plant. This observation hints at a potential synergistic effect, where the combined action of these compounds may yield a more potent antibacterial effect compared to using phenolic acids in isolation. Moreover, both flavonoids and phenolic acids displayed their prowess as reducing agents in synthesis process of AgNPs, contributing to the formation of stable nanoparticles with controlled size and shape (Dakal et al., 2016). This assertion finds confirmation in alluring allure of SR@AgNPs, boasting nanoparticles of uniform diameter at a mesmerizing 92.3 nm. On the other hand, synthesis of WR@AgNPs graced us with a revelation of extraordinary proportions of bimodal size distribution. These findings shed light on coexistence of two distinct particle populations, each proudly showcasing its unique size at 62.2 nm and 111.64 nm. The acquired findings align harmoniously with Lombardo et al.'s seminal work (Lombardo et al., 2016), underscoring that synthesis of silver nanocomposites with a nonuniform size and aggregation yielded the lowest antibacterial activity against *E. coli* and *S. aureus* compared to monodisperse counterpart. Further insight from Dal Lago et al. (Dal Lago et al., 2011) unveiled a compelling revelation smaller silver particles exhibited heightened bactericidal prowess compared to their larger counterparts, with distinct responses witnessed across diverse bacterial strains. From this wealth of data, a compelling conclusion emerges: impact on bacterial cells extends beyond the chemical profile that can potentially modify AgNPs' surface properties. The uniformity of size and diameters of AgNPs appears to play a pivotal role in affecting bacterial response. However, a unique perspective emerges when considering yeast *Rhodotorula glutinis*; it seems to be uniquely influenced solely by the reduction agents present.

3.6. DFT optimization

Optimized structures of targeted molecules extracted from water and solid residues of *Rosmarinus tournefortii* de Noé, along with their interactions with AgNPs, are presented in Fig. 6. In every instance, confirmation of reaching the lowest energy state was validated by the absence of any imaginary frequency. Initially, the calculation of molecular electrostatic potential (MEP) was conducted to predict the locations susceptible to electrophilic and nucleophilic reactions within the molecules under investigation. The distribution of charge in carbohydrate molecules is predominantly influenced by oxygen atoms due to their lone pairs. Notably, carboxylic group within homoplantaginin exhibited the most electronegative potential, implying a strong affinity for attracting electron-deficient species. Oxygen atoms, being highly active have the ability to donate electron density to silver atoms. This suggests plausibility of transferring an electron to a silver atom, thereby transforming an Ag^{+} cation into Ag^{0} and completing $5s^{2}$ and 4 d^{9} orbitals. To substantiate this concept, various Ag_1-complexes were constructed by altering the positioning of silver relative to oxygen atom within the examined molecules. The silver clusters self-arranged to maximize interactions with molecules (He and Zeng, 2010). Based on resulting energy evaluations, the most stable complexes emerged when oxygen atom was positioned near carboxylic group. Consequently, this same configuration was adopted for subsequent investigations.

Referring to He and Zeng's findings, strategic placement of silver atom and clusters was established in close proximity to carboxyl group, a pivotal center within the carbohydrate molecules. This configuration resulted in complexes assuming the lowest energy state. Previous investigations into reactivity patterns indicated that the primary interaction between bioactive compounds and the silver ion predominantly occurred through carboxylic acid or hydroxyl groups (Al-Otaibi et al., 2023). For this interaction to occur, both atoms (Ag and O) must be in contact, underscoring the significance of distance between silver cluster atoms and carbohydrate molecule in comprehending these systems (Gallegos et al., 2022). Within complex formations, distances wield considerable influence and provide insights into nature of interactions. Among the one-silver-atom complexes, interaction energies were notably elevated, ranging from 158 to 269 kcal/mol. However, these complexes exhibited notably elongated Ag–O distances, indicating a relatively weaker interaction due to limited number of silver atoms involved. Conversely, Ag_3-complexes exhibited slightly lower energies (ranging from 130 to 239 kcal/mol) yet showcased shorter Ag–O distances. This indicates that complexes formed with three-silver-atom clusters are thermodynamically preferred over those involving a single silver atom. As the complexes increase in number of silver atoms, distances tend to approach an average length, consequently resulting in a decrease in interaction energies. The disparities in energy values and Ag–O distances are primarily governed by specific type of carbohydrate utilized, ultimately driving improved interactions and formation of more stabilized complexes.

Based on our investigation, a silver nanoparticle composed of 3 silver atoms is anticipated to possess superior attributes owing to its enhanced stability in contrast to smaller nanoparticles. The most stable configuration of three-silver-atom cluster in contact with bioactive molecule exhibits uniform bond lengths measuring 2.73 Å and is characterized by a 58.7° angle. Fig. 7 illustrates the optimized energies of individual molecules, isolated silver atoms and resultant complexes. Notably, silver cluster specifically Ag_3 interact-

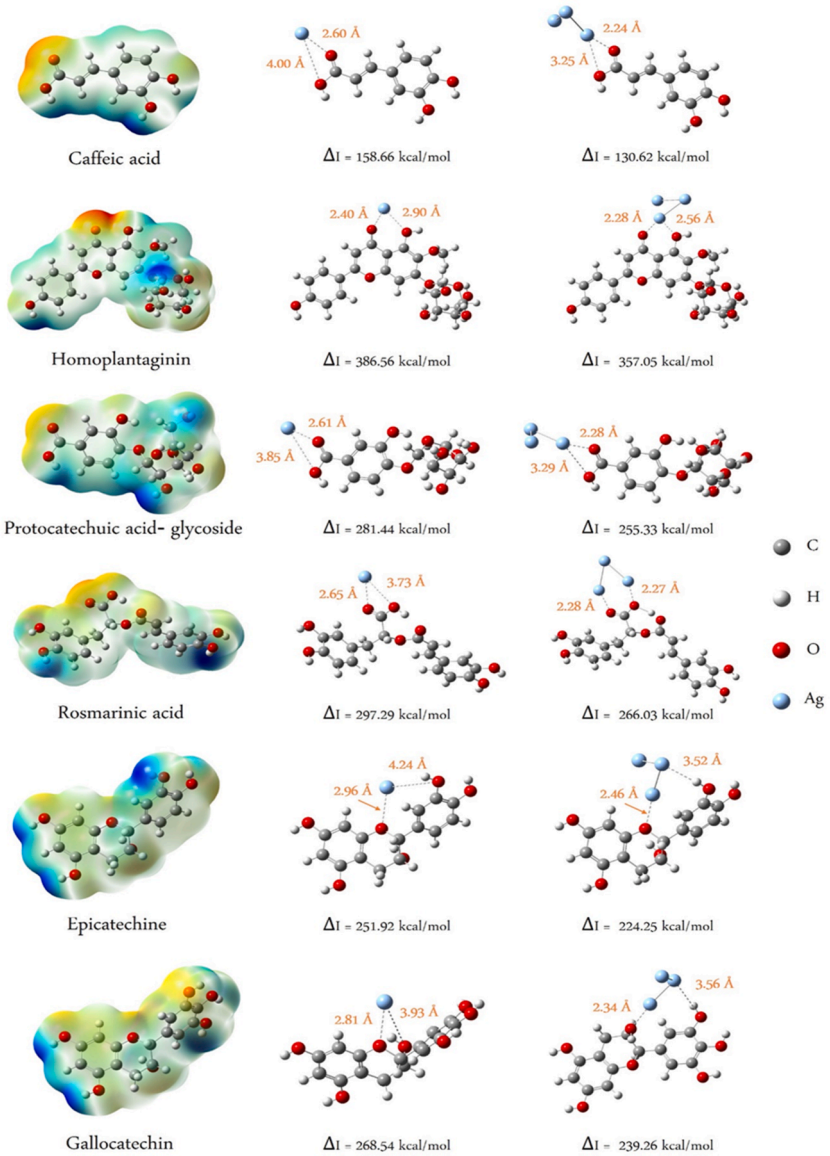

Fig. 6. Optimized geometries with the molecular electrostatic potential maps of selected compounds with and without the inclusion of silver clusters. The interaction energies of target molecules with Ag_1 or Ag_3 are included.

ing with biological molecule exhibited heightened stability in comparison to either standalone silver nanoparticle or isolated biological molecule, as indicated by lower energy levels. Comparing the target molecules, complexes formed between Ag_3 and homoplantaginin, protocatechuic acid-glycoside, and rosmarinic acid exhibit the most substantial interaction energies, measuring 357.05, 255.33, and 266.03 kcal/mol, respectively. This indicates a favourable binding between three-silver-atom clusters and these specific molecules, underpinned by the presence of electrostatic interactions (Kusumaningsih et al., 2023). Significantly, these molecules also manifest shortest Ag–O distances among all compounds, averaging around 2.2–2.3 Å. Furthermore, a low bond distance of approximately 2.2 Å between silver atom and carbonyl functional group of caffeic acid was demonstrated. Notably, Ag–O distances for all four compounds (caffeic acid, homoplantaginin, protocatechuic acid-glycoside and rosmarinic acid) closely align with a typical oxygen-silver bond distance of approximately 2.20–2.35 Å (Njogu et al., 2017). Consequently, these molecules are anticipated to exhibit enhanced reducing activity and offer a high potential for promoting stability of AgNPs.

3.7. Challenges and future outlook

An emerging beacon of hope in biomedical applications lies in realm of green nanoparticles, representing a promising alternative to conventional approaches. These nanoparticles, derived from natural sources or synthesized through eco-friendly methods, offer a sustainable avenue for advancing healthcare solutions. Embracing the principles of environmental consciousness, green nanoparticles present a harmonious fusion of efficacy and ecological responsibility (Shreyash et al., 2021). As they make their debut on biomedical

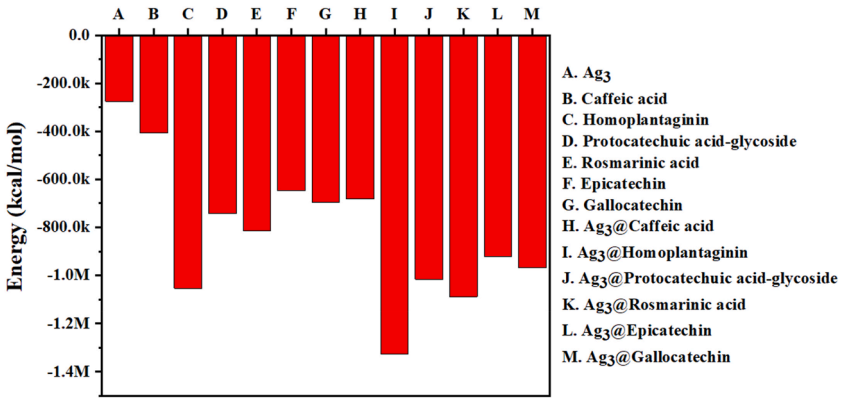

Fig. 7. Total energies of selected compounds with and without inclusion of silver clusters.

stage, their potential shines through in various domains, from drug delivery to diagnostics, tissue engineering and beyond (Sher et al., 2024). These eco-conscious nanoparticles not only demonstrate biomedical prowess but also carry the potential to alleviate concerns regarding environmental impact of traditional nanoparticle synthesis (Selmani et al., 2022). By embracing synergy between innovation and sustainability, green nanoparticles beckon a transformative era in biomedical research and applications, where medical progress goes hand in hand with ecological stewardship. Dynamic attributes inherent to AgNPs embedded within both solid and water residues derived from steam distillation of rosemary have been successfully demonstrated. However, an intriguing challenge arises concerning the synthesis of ZnNPs and CuNPs. Despite exhaustive analysis, including an assessment of their biological activities, successful synthesis has proven elusive. This phenomenon could potentially be ascribed to complex interactions between phenolic compounds and stabilization of CuNPs and ZnNPs. While the developed nanoparticles exhibit remarkable efficiency, there are pertinent issues that demand future attention. In the subsequent sections, delving into these challenges and offering insightful perspectives for further exploration.

3.7.1. Alternative complexation agents for surface modifications

The biosynthesis of metallic nanoparticles is a multifaceted process influenced by various factors such as light exposure, plant extract composition, enzymes, metal ion concentration and reaction conditions, collectively shaping the mechanism, synthesis rate and final particle morphology (El-Seedi et al., 2019). This collaborative amalgamation of influences defines bio-synthesis journey, offering potential for process refinement and customization of nanoparticles for specific applications. Within this realm, a harmonious interplay exists between chemical-reducing agents and latent potential of medicinal plants. Polysaccharides like β-D-glucose and starch serve as eco-conscious reducing agents, demonstrating biocompatibility and water solubility, thus eliminating the need for hazardous solvents (Damiri et al., 2023). Various plant components, including stems, flowers, leaves and seeds, showcase inherent reducing abilities (Alshameri and Owais, 2022). In scenarios where medicinal plants alone may not suffice for metal ion reduction, chemical-reducing agents such as $NaBH_4$ emerge as viable alternatives due to their economic viability, reproducibility, consistent particle size distribution and straightforward experimental protocols. This strategic convergence of medicinal plants' resources with the precision of chemical agents forms a synergistic approach, harnessing both their inherent capabilities and the reliability of chemical-reducing agents.

Shervani et al. (Shervani and Yamamoto, 2011) conducted a comprehensive exploration for synthesis of gold (Au) nanoparticles, delving into influence of various reducing agents, encompassing both traditional chemical methods and environmentally friendly alternatives. The researchers skillfully combined agents such as $NaBH_4$ and β-D-glucose, thereby refining craftsmanship of AuNPs. This holistic approach unveiled an intriguing synergy among these components, orchestrating the transformation of Au salts into monodispersed AuNPs characterized by a distinctive and enchanting wine-red hue a hallmark of their successful formation (Shervani and Yamamoto, 2011). In their methodology, soluble starch and β-D-glucose played crucial roles as carbohydrates in synthesis process. The study highlighted successful production of monodispersed Ag(0) nanoparticles, with a diameter of 15 nm, achieved by reducing $AgNO_3$ precursor salt in a starch-water gel with β-D-glucose (Shervani and Yamamoto, 2011). The investigation into Au(0) metallic nanoparticles revealed nuanced impact of reducing agent type, quantity and solution pH on the size and morphology of nanoparticles. Notably, $NaBH_4$ at 4 equivalents produced the smallest metallic particles (5.3 nm). However, an excess of $NaBH_4$ led to nanoparticles settling out as a precipitate, forming a mesh or wire structure (Shervani and Yamamoto, 2011). This meticulous exploration of synthesis conditions and their effects underscores precision required in the production of metallic nanoparticles with specific size and morphology characteristics.

Another noteworthy endeavour was undertaken by Bikdeloo et al. (2021), employing two reduction agents, $NaBH_4$ and green rosemary extract, to successfully synthesize copper nanoparticles with a hydrodynamic diameter within the range of 50 nm. The reduction of Cu salt by $NaBH_4$ unfolded as a direct and uncomplicated process. Upon introducing $NaBH_4$ into a dispersion of rosemary extract containing Cu precursor salt, electrons and hydrogen converged, setting the stage for reduction of Cu salt, ultimately transforming it into lustrous metallic Cu (Bikdeloo et al., 2021). Throughout this intricate orchestration, rosemary extract played a pivotal dual role, functioning as both a reducing and stabilizing agent, underscoring intricate harmony within this endeavour.

Delving deeper into innovation, realm of mental association opens an alternative pathway for achieving advanced nanocomposite stabilization while harnessing the reduction capabilities of medicinal plants (Kunwar et al., 2023). The combination of metals (Cu, Zn and Ag) introduces unique reduction reagents, creating nanocomposites with enhanced stability. This dynamic approach reinforces structural integrity by seamlessly incorporating stabilizing agents, counteracting agglomeration, and facilitating robust bonds between functional groups and metal ions. The intricate interplay of surface interactions extends to surface modifications, empowering nanocomposites with adaptability, enhanced dispersibility, amplified interactions and heightened biocompatibility. This strategic evolution equips nanocomposites to bridge disciplinary gaps, aligning with dynamic demands (Zhang et al., 2023).

3.7.2. Multifaceted mechanisms of AgNPs toxicity and nanoparticle interactions in inflammation

Nano-silver toxicity manifests through various mechanisms at different levels, encompassing organ, cellular and subcellular dimensions. At organ level, nano-silver can enter the body through various exposure pathways, spreading to vital organs such as the heart, liver, kidney, brain, testes and ovaries, thereby potentially triggering organ-specific pathophysiological effects (Zhang et al., 2022). On cellular plane, nano silver engages with membrane proteins, triggers signaling pathways and disrupts cellular metabolism. Additionally, it generates reactive oxygen species (ROS), inflicts DNA damage, and upregulates autophagy, culminating in cell apoptosis (Attarilar et al., 2020). The cytotoxicity of nano silver is intricately linked to factors such as particle size, concentration, exposure duration and the presence of stabilizers. Delving into subcellular intricacies, nano silver exerts influences on lysosomal activity, inhibits the expression of transcription factor EB (TFEB) and disrupts the normal functioning of lysosomes. Furthermore, it interferes with ion channels on the cell membrane, creating an imbalance in cell membrane potential and leading to cell necrosis (Mehnath et al., 2021).

Shifting focus to inflammation, an immediate response to internal injury, infection, or external factors involves a nuanced interplay of immune cells and signals. Dysregulation in these signals triggers inflammation, prompting recruitment of macrophages, killer cells and stem cells (Fagiani et al., 2022). Macrophages, pivotal in regulating inflammation, manifest in two phenotypes: pro-inflammatory M1 and anti-inflammatory M2. During inflammation, macrophages engulf cellular debris and foster inflammation through the production of activation signals like extracellular matrix proteins, lipopolysaccharide (LPS) and cytokines. Neutrophils, in response to inflammation, migrate to the site, produce pro-inflammatory mediators and attract macrophages (Niu et al., 2021). Upon entering the body, metal nanoparticles (NPs) encounter blood plasma proteins, resulting in the formation of a protein corona around NP (Fig. 8). This corona, comprising proteins like immunoglobulin G (IgG), immunoglobulin M (IgM) and fibrinogen, crucial in natural inflammatory process, is intricately shaped by NP properties (Bashiri et al., 2023). Serum proteins, displaying a strong attraction, play a significant role in forming protein corona, which determines external appearance of NP and gives it a biological identity. This identity then governs NP's movement and its interaction with various chemical reactions.

NPs gain entry into cells through pores or ion channels in the cell membrane, with uptake influenced by their size. Adhesive interactions, driven by electrostatic, van der Waals, or steric forces, orchestrate cellular uptake (Agarwal et al., 2019). The interaction between protein-coated metal NPs and macrophages or neutrophils at inflammatory sites is facilitated by the protein corona, primarily comprised of serum proteins (Cai and Chen, 2019). This protein corona acts as a ligand for receptors on anti-inflammatory M2 macrophages, triggering their activation. This activation amplifies NP uptake, with M2 macrophages exhibiting heightened and swifter NP uptake compared to M1 macrophages in the presence of serum proteins. Neutrophils, responding to stimuli, form extracellular traps (NETs), ensnaring gold nanoparticles within these NETs. This intricate mechanism underscores pivotal role of NPs in modulating inflammatory responses and their dynamic interactions with immune cells.

3.7.3. Harnessing rosmarinic acid nanoparticles for inflammatory conditions

Inflammatory bowel disease (IBD), a complex and recurrent condition with an unknown aetiology, demands increased attention as a critical public health concern. Classified into two major subtypes, Crohn's disease (CD) and ulcerative colitis (UC), UC specifically manifests as a chronic inflammatory disorder of rectum and colon (Kaplan and Windsor, 2021). Addressing the intricate nature of IBD, Chung et al.'s ground-breaking study explores the potential of PEGylated rosmarinic acid nanoparticles (RANPs) derived from rosemary extract as a nanomedicine for IBD treatment (Chung et al., 2020). With a diameter of 63.5 $\pm$ 4.0 nm, RANPs exhibit superior therapeutic efficacy, synergizing with conventional medication, scavenging reactive oxygen species (ROS) and protecting against oxidative damage. In a mouse model of acute colitis, RANPs treatment at doses of 20 mg/kg and 30 mg/kg significantly reduces body weight loss, bloody stools and disease activity index (DAI) scores, indicating a substantial decrease in inflammation and damage to colon. Histological analysis further reveals the restoration of colon lining structure and attenuation of inflammation (Chung et al., 2020). Additionally, RANPs dose-dependently attenuate colonic muscle thickening, supporting their role in reducing inflammation and damage to the colon. Mechanistically, RANPs inhibit activation of pro-inflammatory transcription factors NF-κB and STAT3 and attenuate neutrophil infiltration in the inflamed colon (Chung et al., 2020). Loading the corticosteroid medication DEX into RANPs enhances therapeutic efficacy, demonstrating greater reductions in DAI scores and colon shortening compared to bare RANPs. Importantly, RANPs exhibit good biocompatibility both in vitro and in vivo, positioning them as a promising therapeutic nanomedicine for various inflammatory diseases, including IBD. This provides visual evidence of the therapeutic effects of experimental modalities on colitis-associated tissue damage and inflammation.

Relating to the broader context of inflammatory conditions, study seamlessly aligns with investigations into rheumatoid arthritis (RA). Recognizing RA's enduring challenge to global public health, Lu et al.'s (Luca et al., 2023) research explores antioxidative nanomedicine using ribonucleoproteins (RNPs) derived from a natural polyphenol-based compound. The study's schematic illustration delineates the fabrication process of RNPs (RosA nanoparticles) and reveals their therapeutic mechanism against RA. Synthesized through self-assembling oxidative oligomerization of RosA, RNPs play a crucial role in alleviating oxidative stress in RA joints, scav-

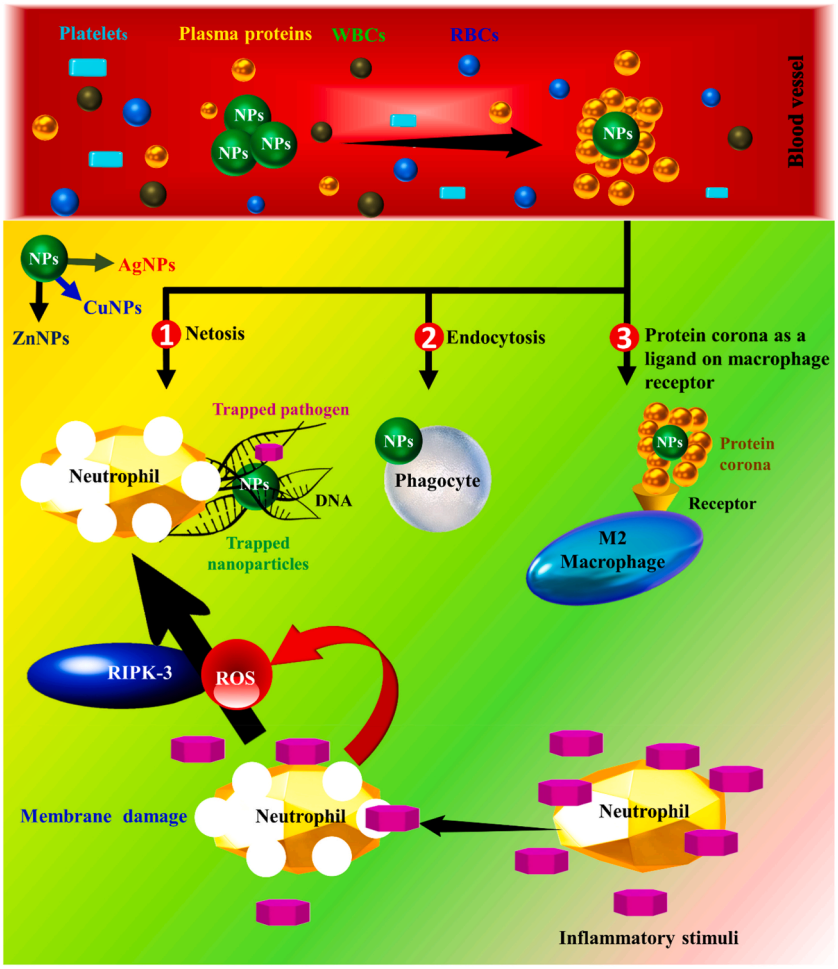

Fig. 8. Different nanoparticles employ anti-inflammatory mechanisms. Adopted from (Agarwal et al., 2019). Copyright Elsevier ©2018.

enging ROS, elevating anti-inflammatory M2 subtype through macrophage polarization and augmenting the production of anti-inflammatory cytokines (Lu et al., 2023). The RNPs exhibit the ability to inhibit synovitis, angiogenesis, cartilage degradation and bone erosion, as evidenced by reduced clinical scores, ankle-joint thickness and inflammation in the RNPs-treated group compared to the RosA-treated group.

The study provides insights into the cellular uptake of RNPs, emphasizing their rapid internalization within hours by cells (Lu et al., 2023). The fluorescence imaging analysis showcases the presence of RNPs in both the nuclei and cytoplasm of RAW 264.7 cells, indicating efficient cellular uptake. In vivo, biodistribution studies further underscore the excellent targeting ability of RNPs, with enhanced accumulation at inflammatory joints observed in fluorescence imaging of the paws of rats with collagen-induced arthritis (CIA). This seamless connection between studies reveals a common thread in addressing inflammatory conditions through nanomedicine, offering innovative and targeted therapeutic approaches.

4. Conclusions

The utilization of by-products generated from *Rosmarinus tournefortii* de Noé steam distillation as metal-reducing agents in the green synthesis of nanoparticles offers a promising route for sustainable and environmentally friendly nanomaterial production. These nanoparticles, whether sourced naturally or synthesized ecologically, exceed efficacy norms while embracing environmental responsibility. The synthesized nanoparticles underwent comprehensive characterization using UV–vis, XRD, FTIR, SEM/EDX and Zeta analysis. The study successfully enhanced the synthesis of AgNPs using two distinct by-products, water and solid residues. However, ZnNPs and CuNPs synthesis encountered limitations, as indicated by spectroscopic characterization. Factors such as inadequate synthesis conditions, nanoparticle oxidation, agglomeration during synthesis and the absence of appropriate surface ligands or stabilizing agents may have contributed to these challenges. The average crystallite size of AgNPs was found to be 17.98 and 18.49 nm for SR@Ag and WR@Ag composites, respectively, with stable and negative Zeta potential values (ζ values: −22.8 and −17.2 mV), suggesting nanoparticle stability. Both types of by-products yielded nanoparticles with predominantly spherical morphology, featuring varying nanoscale diameters. Antioxidant assessment favoured water residue, showing consistent scavenging inhibition

(94.9–97.3%) across concentrations, while antimicrobial activity against Gram-negative, Gram-positive bacteria and yeast *Rhodotorula glutinis* was notably enhanced. Furthermore, DFT analysis unveiled significant interactions among homoplantaginin, rosmarinic acid, protocatechuic acid-glycoside and caffeic acid, resulting in heightened reduction activity of AgNPs. These interactions exhibited substantial energy values, measuring 357.05, 266.03, 255.33 and 130.62 kcal/mol, respectively. These findings collectively advance the understanding of green nanoparticle synthesis, paving the way for further innovation and applications in diverse fields. Challenges and opportunities persist, including the pursuit of alternative complexation agents for surface modification. Shifting focus, the section explores the multifaceted toxicity mechanisms of silver nanoparticles at organ, cellular and subcellular levels, emphasizing their intricate interactions with inflammation processes. Additionally, it introduces two promising nanomedicine approaches one involving PEGylated rosmarinic acid nanoparticles, a compound derived from rosemary extract, for treating inflammatory bowel disease and another utilizing ribonucleoprotein for addressing rheumatoid arthritis. These findings underscore the potential of nanotechnology, particularly harnessing rosemary-derived compounds like rosmarinic acid, in innovative and targeted therapeutic interventions for diverse inflammatory conditions.

CRediT authorship contribution statement

Imane Ziani: Writing – review & editing, Software, Investigation, Formal analysis, Data curation, Conceptualization. **Abdelqader El Guerraf:** Writing – review & editing, Investigation. **Nour Eddine Bentouhami:** Writing – review & editing, Visualization. **Mohamed Brahmi:** Writing – review & editing. **Hamza Bouakline:** Writing – review & editing. **Ali El Bachiri:** Writing – review & editing, Investigation. **Marie-Laure Fauconnier:** Writing – review & editing, Supervision, Project administration. **Sabah Ansar:** Writing – review & editing, Funding acquisition. **Farooq Sher:** Writing – review & editing, Supervision, Project administration, Funding acquisition.

Declaration of competing interest

The authors declare that they have no known competing financial interests or personal relationships that could have appeared to influence the work reported in this paper.

Data availability

Data will be made available on request.

Acknowledgements

The authors extend their genuine gratitude to Cluster Valbiom Maroc and the International Society of Engineering Science and Technology (ISEST) UK for the financial support provided. A. El Guerraf acknowledges financial support from the Czech Science Foundation (GACR), project 22-23407S. The authors are also thank the Researchers Supporting Project number (RSP2024R169), King Saud University, Riyadh, Saudi Arabia for the financial support.

References

Abdollahzadeh, E., Nematollahi, A., Hosseini, H., 2021. Composition of antimicrobial edible films and methods for assessing their antimicrobial activity: a review. Trends Food Sci. Technol. 110, 291–303. https://doi.org/10.1016/j.tifs.2021.01.084.

Adra, H.J., Lim, D., Kim, H., Jeong, K., Luo, K., Kim, Y.-R., 2024. Precision-controlled synthesis of monodisperse starch nanoparticles: factors affecting the self-assembly kinetics. Food Hydrocolloids 110081. https://doi.org/10.1016/j.foodhyd.2024.110081.

Agarwal, H., Nakara, A., Shanmugam, V.K., 2019. Anti-inflammatory mechanism of various metal and metal oxide nanoparticles synthesized using plant extracts: a review. Biomed. Pharmacother. 109, 2561–2572. https://doi.org/10.1016/j.biopha.2018.11.116.

Al-Otaibi, J.S., Mary, Y Sheena, Mary, Y Shyma, Krátký, M., Vinsova, J., Gamberini, M.C., 2023. DFT, TD-DFT and SERS analysis of a bioactive benzohydrazide's adsorption in silver hydrosols at various concentrations. J. Mol. Liq. 373, 121243. https://doi.org/10.1016/j.molliq.2023.121243.

Almela, L., Sánchez-Muñoz, B., Fernández-López, J.A., Roca, M.J., Rabe, V., 2006. Liquid chromatograpic-mass spectrometric analysis of phenolics and free radical scavenging activity of rosemary extract from different raw material. J. Chromatogr. A 1120, 221–229. https://doi.org/10.1016/j.chroma.2006.02.056.

Alshameri, A.W., Owais, M., 2022. Antibacterial and cytotoxic potency of the plant-mediated synthesis of metallic nanoparticles Ag NPs and ZnO NPs: a Review. OpenNano 8, 100077. https://doi.org/10.1016/j.onano.2022.100077.

Attarilar, S., Yang, Jinfan, Ebrahimi, M., Wang, Q., Liu, J., Tang, Y., Yang, Junlin, 2020. The toxicity phenomenon and the related occurrence in metal and metal oxide nanoparticles: a brief review from the biomedical perspective. Front. Bioeng. Biotechnol. 8, 822. https://doi.org/10.3389/fbioe.2020.00822.

Barbieri, J.B., Goltz, C., Cavalheiro, F.B., Toci, A.T., Igarashi-Mafra, L., Mafra, M.R., 2020. Deep eutectic solvents applied in the extraction and stabilization of rosemary (Rosmarinus officinalis L.) phenolic compounds. Ind. Crops Prod. 144, 112049. https://doi.org/10.1016/j.indcrop.2019.112049.

Bashiri, G., Padilla, M.S., Swingle, K.L., Shepherd, S.J., Mitchell, M.J., Wang, K., 2023. Nanoparticle protein corona: from structure and function to therapeutic targeting. Lab Chip 23, 1432–1466. https://doi.org/10.1039/D2LC00799A.

Bendif, H., Boudjeniba, M., Djamel Miara, M., Biqiku, L., Bramucci, M., Caprioli, G., Lupidi, G., Quassinti, L., Sagratini, G., Vitali, L.A., Vittori, S., Maggi, F., 2017. Rosmarinus eriocalyx: an alternative to Rosmarinus officinalis as a source of antioxidant compounds. Food Chem. 218, 78–88. https://doi.org/10.1016/j.foodchem.2016.09.063.

Bereza-Malcolm, L.T., Mann, G., Franks, A.E., 2015. Environmental sensing of heavy metals through whole cell microbial biosensors: a synthetic biology approach. ACS Synth. Biol. 4, 535–546. https://doi.org/10.1021/sb500286r.

Bhutto, A.A., Kalay, Ş., Sherazi, S.T.H., Culha, M., 2018. Quantitative structure–activity relationship between antioxidant capacity of phenolic compounds and the plasmonic properties of silver nanoparticles. Talanta 189, 174–181. https://doi.org/10.1016/j.talanta.2018.06.080.

Bikdeloo, M., Ahsani Irvani, M., Roosta, H.R., Ghanbari, D., 2021. Green synthesis of copper nanoparticles using rosemary extract to reduce postharvest decays caused by botrytis cinerea in tomato. J. Nanostructures 11, 834–841. https://doi.org/10.22052/JNS.2021.04.020.

Borah, R., Ninakanti, R., Nuyts, G., Peeters, H., Pedrazo-Tardajos, A., Nuti, S., Vande Velde, C., De Wael, K., Lenaerts, S., Bals, S., 2021. Selectivity in the ligand functionalization of photocatalytic metal oxide nanoparticles for phase transfer and self-assembly applications. Chem. Eur J. 27, 9011–9021. https://doi.org/10.1002/chem.202100029.

Bouammali, H., Zraibi, L., Ziani, I., Merzouki, M., Bourassi, L., Fraj, E., Challioui, A., Azzaoui, K., Sabbahi, R., Hammouti, B., Jodeh, S., Hassiba, M., Touzani, R., 2023.

Rosemary as a potential source of natural antioxidants and anticancer agents: a molecular docking study. Plants 13, 89. https://doi.org/10.3390/plants13010089.
Cai, R., Chen, C., 2019. The crown and the scepter: roles of the protein corona in nanomedicine. Adv. Mater. 31, 1805740. https://doi.org/10.1002/adma.201805740.
Celano, R., Piccinelli, A.L., Pagano, I., Roscigno, G., Campone, L., De Falco, E., Russo, M., Rastrelli, L., 2017. Oil distillation wastewaters from aromatic herbs as new natural source of antioxidant compounds. Food Res. Int. 99, 298–307. https://doi.org/10.1016/j.foodres.2017.05.036.
Chen, Z., Chen, L., Khoo, K.S., Gupta, V.K., Sharma, M., Show, P.L., Yap, P.S., 2023. Exploitation of lignocellulosic-based biomass biorefinery: a critical review of renewable bioresource, sustainability and economic views. Biotechnol. Adv. 69, 108265. https://doi.org/10.1016/j.biotechadv.2023.108265.
Chung, C.H., Jung, W., Keum, H., Kim, T.W., Jon, S., 2020. Nanoparticles derived from the natural antioxidant rosmarinic acid ameliorate acute inflammatory bowel disease. ACS Nano 14, 6887–6896. https://doi.org/10.1021/acsnano.0c01018.
Da Silva, R.P.F.F., Rocha-Santos, T.A.P., Duarte, A.C., 2016. Supercritical fluid extraction of bioactive compounds. TrAC Trends Anal. Chem. 76, 40–51. https://doi.org/10.1016/j.trac.2015.11.013.
Dakal, T.C., Kumar, A., Majumdar, R.S., Yadav, V., 2016. Mechanistic Basis of Antimicrobial Actions of Silver Nanoparticles, vol. 7. p. 1831. https://doi.org/10.3389/fmicb.2016.01831.
Dal Lago, V., França de Oliveira, L., de Almeida Gonçalves, K., Kobarg, J., Borba Cardoso, M., 2011. Size-selective silver nanoparticles: future of biomedical devices with enhanced bactericidal properties. J. Mater. Chem. 21, 12267–12273. https://doi.org/10.1039/c1jm12297e.
Damiri, F., Fatimi, A., Santos, A.C.P., Varma, R.S., Berrada, M., 2023. Smart stimuli-responsive polysaccharide nanohydrogels for drug delivery: a review. J. Mater. Chem. B 11, 10538–10565. https://doi.org/10.1039/D3TB01712E.
Das, J., Velusamy, P., 2013. Antibacterial effects of biosynthesized silver nanoparticles using aqueous leaf extract of Rosmarinus officinalis L. Mater. Res. Bull. 48, 4531–4537. https://doi.org/10.1016/j.materresbull.2013.07.049.
de Almeida Gonçalves, G., de Sa-Nakanishi, A.B., Comar, J.F., Bracht, L., Dias, M.I., Barros, L., Peralta, R.M., Ferreira, I.C.F.R., Bracht, A., 2018. Water soluble compounds of Rosmarinus officinalis L. improve the oxidative and inflammatory states of rats with adjuvant-induced arthritis. Food Funct. 9, 2328–2340. https://doi.org/10.1039/C7FO01928A.
de Elguea-Culebras, G.O., Panamá-Tapia, L.A., Melero-Bravo, E., Cerro-Ibáñez, N., Calvo-Martínez, A., Sánchez-Vioque, R., 2023. Comparison of the phenolic composition and biological capacities of wastewater from Origanum vulgare L., Rosmarinus officinalis L., Salvia lavandulifolia Vahl. and Thymus mastichina L. resulting from two hydrodistillation systems: clevenger and MAE. J. Appl. Res. Med. Aromat. Plants 34, 100480. https://doi.org/10.1016/j.jarmap.2023.100480.
de Souza Niero, A.L., Possolli, N.M., da Silva, D.F., Demétrio, K.B., Zocche, J.J., de Souza, G.M.S., Dias, J.F., Vieira, J.L., Barbosa, J.D.V., Soares, M.B.P., 2023. Composite beads of alginate and biological hydroxyapatite from poultry and mariculture for hard tissue repair. Ceram. Int. 49, 25319–25332. https://doi.org/10.1016/j.ceramint.2023.05.068.
El-Seedi, H.R., El-Shabasy, R.M., Khalifa, S.A.M., Saeed, A., Shah, A., Shah, R., Iftikhar, F.J., Abdel-Daim, M.M., Omri, A., Hajrahand, N.H., 2019. Metal nanoparticles fabricated by green chemistry using natural extracts: biosynthesis, mechanisms, and applications. RSC Adv. 9, 24539–24559. https://doi.org/10.1039/C9RA02225B.
El Guerraf, A., Jadi, S. Ben, Ziani, I., Dalli, M., Sher, F., Bazzaoui, M., Bazzaoui, E.A., 2023. Multifunctional smart conducting polymers-silver nanocomposites-modified biocellulose fibers for innovative food packaging applications. Ind. Eng. Chem. Res. 62, 4540–4553. https://doi.org/10.1021/acs.iecr.2c01327.
Fagiani, F., Di Marino, D., Romagnoli, A., Travelli, C., Voltan, D., Di Cesare Mannelli, L., Racchi, M., Govoni, S., Lanni, C., 2022. Molecular regulations of circadian rhythm and implications for physiology and diseases. Signal Transduct. Targeted Ther. 7, 41. https://doi.org/10.1038/s41392-022-00899-y.
Farshchi, H.K., Azizi, M., Jaafari, M.R., Nemati, S.H., Fotovat, A., 2018. Green synthesis of iron nanoparticles by Rosemary extract and cytotoxicity effect evaluation on cancer cell lines. Biocatal. Agric. Biotechnol. 16, 54–62. https://doi.org/10.1016/j.bcab.2018.07.017.
Gallegos, F.E., Meneses, L.M., Cuesta, S.A., Santos, J.C., Arias, J., Carrillo, P., Pilaquinga, F., 2022. Computational modeling of the interaction of silver clusters with carbohydrates. ACS Omega 7, 4750–4756. https://doi.org/10.1021/acsomega.1c04149.
Ghaedi, M., Yousefinejad, M., Safarpoor, M., Khafri, H.Z., Purkait, M.K., 2015. Rosmarinus officinalis leaf extract mediated green synthesis of silver nanoparticles and investigation of its antimicrobial properties. J. Ind. Eng. Chem. 31, 167–172. https://doi.org/10.1016/j.jiec.2015.06.020.
Gitipour, A., El Badawy, A., Arambewela, M., Miller, B., Scheckel, K., Elk, M., Ryu, H., Gomez-Alvarez, V., Santo Domingo, J., Thiel, S., Tolaymat, T., 2013. The impact of silver nanoparticles on the composting of municipal solid waste. Environ. Sci. Technol. 47, 14385–14393. https://doi.org/10.1021/es402510a.
Gonçalves, G.A., Corrêa, R.C.G., Barros, L., Dias, M.I., Calhelha, R.C., Correa, V.G., Bracht, A., Peralta, R.M., Ferreira, I.C.F.R., 2019. Effects of in vitro gastrointestinal digestion and colonic fermentation on a rosemary (Rosmarinus officinalis L) extract rich in rosmarinic acid. Food Chem. 271, 393–400. https://doi.org/10.1016/j.foodchem.2018.07.132.
Harsha Haridas, E.S., Bhattacharya, S., Varma, M.K.R., Chandra, G.K., 2023. Bioinspired 5-caffeoylquinic acid capped silver nanoparticles using Coffee arabica leaf extract for high-sensitive cysteine detection. Sci. Rep. 13, 1–12. https://doi.org/10.1038/s41598-023-34944-9.
He, Y., Zeng, T., 2010. First-principles study and model of dielectric functions of silver nanoparticles. J. Phys. Chem. C 114, 18023–18030. https://doi.org/10.1021/jp101598j.
Herrero, Miguel, Plaza, M., Cifuentes, A., Ibáñez, E., 2010. Green processes for the extraction of bioactives from Rosemary: chemical and functional characterization via ultra-performance liquid chromatography-tandem mass spectrometry and in-vitro assays. J. Chromatogr. A 1217, 2512–2520. https://doi.org/10.1016/j.chroma.2009.11.032.
Herrero, M., Plaza, M., Cifuentes, A., Ibáñez, E., 2010. Green processes for the extraction of bioactives from Rosemary: chemical and functional characterization via ultra-performance liquid chromatography-tandem mass spectrometry and in-vitro assays. J. Chromatogr. A 1217, 2512–2520. https://doi.org/10.1016/j.chroma.2009.11.032.
Huh, A.J., Kwon, Y.J., 2011. "Nanoantibiotics": a new paradigm for treating infectious diseases using nanomaterials in the antibiotics resistant era. J. Control. release 156, 128–145.
Jahan, I., Erci, F., Isildak, I., 2021. Facile microwave-mediated green synthesis of non-toxic copper nanoparticles using Citrus sinensis aqueous fruit extract and their antibacterial potentials. J. Drug Deliv. Sci. Technol. 61, 102172. https://doi.org/10.1016/j.jddst.2020.102172.
Jędrzejczyk, R.J., Gustab, M., Ważny, R., Domka, A., Jodłowski, P.J., Sitarz, M., Bezkosty, P., Kowalski, M., Pawcenis, D., Jarosz, K., 2023. Iron inactivation by Sporobolomyces ruberrimus and its potential role in plant metal stress protection. An in vitro study. Sci. Total Environ. 870, 161887. https://doi.org/10.1016/j.scitotenv.2023.161887.
Kaplan, G.G., Windsor, J.W., 2021. The four epidemiological stages in the global evolution of inflammatory bowel disease. Nat. Rev. Gastroenterol. Hepatol. 18, 56–66. https://doi.org/10.1038/s41575-020-00360-x.
Kaushik, V., Kagdada, H.L., Singh, D.K., Pathak, S., 2022. Enhancement of SERS effect in Graphene-Silver hybrids. Appl. Surf. Sci. 574, 151724. https://doi.org/10.1016/j.apsusc.2021.151724.
Kelly, K.L., Coronado, E., Zhao, L.L., Schatz, G.C., 2003. The optical properties of metal nanoparticles: the influence of size, shape, and dielectric environment. J. Phys. Chem. B 107 (3), 668–677. https://doi.org/10.1021/jp026731y.
Kim, D.-Y., Yang, T., Srivastava, P., Nile, S.H., Seth, C.S., Jadhav, U., Syed, A., Bahkali, A.H., Ghodake, G.S., 2024. Alginic acid-functionalized silver nanoparticles: a rapid monitoring tool for detecting the technology-critical element tellurium. J. Hazard Mater. 465, 133161. https://doi.org/10.1016/j.jhazmat.2023.133161.
Kim, Y., Ji, S., Nam, J.-M., 2023. A chemist's view on electronic and steric effects of surface ligands on plasmonic metal nanostructures. Acc. Chem. Res. 56, 2139–2150. https://doi.org/10.1021/acs.accounts.3c00196.
Kotakadi, V.S., Gaddam, S.A., Rao, Y.S., Prasad, T., Reddy, A.V., Gopal, D.V.R.S., 2014. Biofabrication of silver nanoparticles using Andrographis paniculata. Eur. J. Med. Chem. 73, 135–140. https://doi.org/10.1016/j.ejmech.2013.12.004.
Kunwar, S., Roy, A., Bhusal, U., Gacem, A., Abdullah, M.M.S., Sharma, P., Yadav, K.K., Rustagi, S., Chatterjee, N., Deshwal, V.K., 2023. Bio-fabrication of Cu/Ag/Zn nanoparticles and their antioxidant and dye degradation activities. Catalysts 13, 891. https://doi.org/10.3390/catal13050891.
Kusumaningsih, T., Prasetyo, W.E., Istiqomah, A., Firdaus, M., Wibowo, F.R., 2023. Sustainable synthesis of silver nanoparticles with enhanced anticancer, antibacterial, and antioxidant properties mediated by dimeric 2,4-diacetyl phloroglucinol: experimental and computational insights. Surface. Interfac. 36, 102545. https://doi.org/10.1016/j.surfin.2022.102545.
Lee, J., Chae, K.-J., 2021. A systematic protocol of microplastics analysis from their identification to quantification in water environment: a comprehensive review. J.

Hazard Mater. 403, 124049. https://doi.org/10.1016/j.jhazmat.2020.124049.
Liu, T., Sui, X., Zhang, R., Yang, L., Zu, Y., Zhang, L., Zhang, Y., Zhang, Z., 2011. Application of ionic liquids based microwave-assisted simultaneous extraction of carnosic acid, rosmarinic acid and essential oil from Rosmarinus officinalis. J. Chromatogr. A 1218, 8480–8489. https://doi.org/10.1016/j.chroma.2011.09.073.
Lombardo, P.C., Poli, A.L., Castro, L.F., Perussi, J.R., Schmitt, C.C., 2016. Photochemical deposition of silver nanoparticles on clays and exploring their antibacterial activity. ACS Appl. Mater. Interfaces 8, 21640–21647. https://doi.org/10.1021/acsami.6b05292.
Lu, B., Li, C., Jing, L., Zhuang, F., Xiang, H., Chen, Y., Huang, B., 2023. Rosmarinic acid nanomedicine for rheumatoid arthritis therapy: targeted RONS scavenging and macrophage repolarization. J. Contr. Release 362, 631–646. https://doi.org/10.1016/j.jconrel.2023.09.012.
Luca, S.V., Zengin, G., Sinan, K.I., Korona-Glowniak, I., Minceva, M., Skalicka-Woźniak, K., Trifan, A., 2023. Value-added compounds with antimicrobial, antioxidant, and enzyme-inhibitory effects from post-distillation and post-supercritical CO2 extraction by-products of rosemary. Antioxidants 12, 244. https://doi.org/10.3390/antiox12020244.
Lv, Z., He, S., Wang, Y., Zhu, X., 2021. Noble metal nanomaterials for NIR-triggered photothermal therapy in cancer. Adv. Healthcare Mater. 10, 2001806. https://doi.org/10.1002/adhm.202001806.
Mahdi, M.A., Yousefi, S.R., Jasim, L.S., Salavati-Niasari, M., 2022. Green synthesis of DyBa2Fe3O7. 988/DyFeO3 nanocomposites using almond extract with dual eco-friendly applications: photocatalytic and antibacterial activities. Int. J. Hydrogen Energy 47, 14319–14330. https://doi.org/10.1016/j.ijhydene.2022.02.175.
Martins, T.A.G., Falconi, I.B.A., Pavoski, G., de Moraes, V.T., Galluzzi Baltazar, M., dos, P., Espinosa, D.C.R., 2021. Green synthesis, characterization, and application of copper nanoparticles obtained from printed circuit boards to degrade mining surfactant by Fenton process. J. Environ. Chem. Eng. 9, 106576. https://doi.org/10.1016/j.jece.2021.106576.
Mehnath, S., Das, A.K., Verma, S.K., Jeyaraj, M., 2021. Biosynthesized/green-synthesized nanomaterials as potential vehicles for delivery of antibiotics/drugs. In: Comprehensive Analytical Chemistry, first ed., vol. 94. Elsevier, pp. 363–432. https://doi.org/10.1016/bs.coac.2020.12.011.
Miljanović, A., Dent, M., Grbin, D., Pedisić, S., Zorić, Z., Marijanović, Z., Jerković, I., Bielen, A., 2023. Sage, rosemary, and bay laurel hydrodistillation by-products as a source of bioactive compounds. Plants 12 (13), 2394. https://doi.org/10.3390/plants12132394.
Mittal, A.K., Chisti, Y., Banerjee, U.C., 2013. Synthesis of metallic nanoparticles using plant extracts. Biotechnol. Adv. 31, 346–356. https://doi.org/10.1016/j.biotechadv.2013.01.003.
Mohamad Sukri, S.N.A., Shameli, K., Teow, S.Y., Chew, J., Ooi, L.T., Lee-Kiun Soon, M., Ismail, N.A., Moeini, H., 2023. Enhanced antibacterial and anticancer activities of plant extract mediated green synthesized zinc oxide-silver nanoparticles. Front. Microbiol. 14, 1–14. https://doi.org/10.3389/fmicb.2023.1194292.
Naghdi, M., Ghovvati, M., Rabiee, N., Ahmadi, S., Abbariki, N., Sojdeh, S., Ojaghi, A., Bagherzadeh, M., Akhavan, O., Sharifi, E., 2022. Magnetic nanostructures in nanomedicine revolution: a review of growing magnetic nanocomposites in biomedical applications. Adv. Colloid Interface Sci. 308, 102771. https://doi.org/10.1016/j.cis.2022.102771.
Niu, Y., Wang, Z., Shi, Y., Dong, L., Wang, C., 2021. Modulating macrophage activities to promote endogenous bone regeneration: biological mechanisms and engineering approaches. Bioact. Mater. 6, 244–261. https://doi.org/10.1016/j.bioactmat.2020.08.012.
Njogu, E.M., Omondi, B., Nyamori, V.O., 2017. Coordination polymers and discrete complexes of Ag (I)-N-(pyridylmethylene) anilines: synthesis, crystal structures and photophysical properties. J. Coord. Chem. 70, 2796–2814. https://doi.org/10.1080/00958972.2017.1370088.
Noukelag, S.K., Razanamahandry, L.C., Ntwampe, S.K.O., Arendse, C.J., Maaza, M., 2021. Industrial dye removal using bio-synthesized Ag-doped ZnO nanoparticles. Environ. Nanotechnol. Monit. Manag. 16, 100463. https://doi.org/10.1016/j.enmm.2021.100463.
Oliveira, A.L.S., Gondim, S., Gómez-García, R., Ribeiro, T., Pintado, M., 2021. Olive leaf phenolic extract from two Portuguese cultivars –bioactivities for potential food and cosmetic application. J. Environ. Chem. Eng. 9, 106175. https://doi.org/10.1016/j.jece.2021.106175.
Piñeros-Hernandez, D., Medina-Jaramillo, C., López-Córdoba, A., Goyanes, S., 2017. Edible cassava starch films carrying rosemary antioxidant extracts for potential use as active food packaging. Food Hydrocolloids 63, 488–495. https://doi.org/10.1016/j.foodhyd.2016.09.034.
Pisoschi, A.M., Iordache, F., Stanca, L., Gajaila, I., Ghimpeteanu, O.M., Geicu, O.I., Bilteanu, L., Serban, A.I., 2022. Antioxidant, anti-inflammatory, and immunomodulatory roles of nonvitamin antioxidants in anti-SARS-CoV-2 therapy. J. Med. Chem. 65, 12562–12593. https://doi.org/10.1021/acs.jmedchem.2c01134.
Pryshchepa, O., Pomastowski, P., Buszewski, B., 2020. Silver nanoparticles: synthesis, investigation techniques, and properties. Adv. Colloid Interface Sci. 284, 102246. https://doi.org/10.1016/j.cis.2020.102246.
Rabiee, N., Bagherzadeh, M., Kiani, M., Ghadiri, A.M., 2020. Rosmarinus officinalis directed palladium nanoparticle synthesis: investigation of potential anti-bacterial, anti-fungal and Mizoroki-Heck catalytic activities. Adv. Powder Technol. 31, 1402–1411. https://doi.org/10.1016/j.apt.2020.01.024.
Rambabu, K., Bharath, G., Banat, F., Show, P.L., 2021. Green synthesis of zinc oxide nanoparticles using Phoenix dactylifera waste as bioreductant for effective dye degradation and antibacterial performance in wastewater treatment. J. Hazard Mater. 402, 123560. https://doi.org/10.1016/j.jhazmat.2020.123560.
Rao, B.R., Kumar, R., Haque, S., Kumar, J.M., Rao, T.N., Kothapalli, R.V.S.N., Patra, C.R., 2021. Ag2 [fe (cn) 5no]-fabricated hydrophobic cotton as a potential wound healing dressing: an in vivo approach. ACS Appl. Mater. Interfaces 13, 10689–10704. https://doi.org/10.1021/acsami.0c19904.
Raut, R.W., Mendhulkar, V.D., Kashid, S.B., 2014. Photosensitized synthesis of silver nanoparticles using Withania somnifera leaf powder and silver nitrate. J. Photochem. Photobiol. B Biol. 132, 45–55. https://doi.org/10.1016/j.jphotobiol.2014.02.001.
Sankaran, R., Markandan, K., Khoo, K.S., Cheng, C.K., Ashokkumar, V., Deepanraj, B., Show, P.L., 2021. The expansion of lignocellulose biomass conversion into bioenergy via nanobiotechnology. Front. Nanotechnol. 3, 1–10. https://doi.org/10.3389/fnano.2021.793528.
Scroccarello, A., Junior, B.M.-H., Della Pelle, F., Ciancetta, J., Ferraro, G., Fratini, E., Valbonetti, L., Copez, C.C., Compagnone, D., 2021. Effect of phenolic compounds-capped AgNPs on growth inhibition of Aspergillus Niger. Colloids Surfaces B Biointerfaces 199, 111533. https://doi.org/10.1016/j.colsurfb.2020.111533.
Selmani, A., Kovačević, D., Bohinc, K., 2022. Nanoparticles: from synthesis to applications and beyond. Adv. Colloid Interface Sci. 303, 102640. https://doi.org/10.1016/j.cis.2022.102640.
Sher, F., Ziani, I., Smith, M., Chugreeva, G., Hashimzada, S.Z., Prola, L.D.T., Sulejmanović, J., Sher, E.K., 2024. Carbon quantum dots conjugated with metal hybrid nanoparticles as advanced electrocatalyst for energy applications–A review. Coord. Chem. Rev. 500, 215499. https://doi.org/10.1016/j.ccr.2023.215499.
Shervani, Z., Yamamoto, Y., 2011. Carbohydrate-directed synthesis of silver and gold nanoparticles: effect of the structure of carbohydrates and reducing agents on the size and morphology of the composites. Carbohydr. Res. 346, 651–658. https://doi.org/10.1016/j.carres.2011.01.020.
Shreyash, N., Bajpai, S., Khan, M.A., Vijay, Y., Tiwary, S.K., Sonker, M., 2021. Green synthesis of nanoparticles and their biomedical applications: a review. ACS Appl. Nano Mater. 4, 11428–11457. https://doi.org/10.1021/acsanm.1c02946.
Tariq, G.H., Asghar, G., Shifa, M.S., Anis-Ur-Rehman, M., Ullah, S., Shah, Z.A., Ziani, I., Tawfeek, A.M., Sher, F., 2023. Effect of copper doping on plasmonic nanofilms for high performance photovoltaic energy applications. Phys. Chem. Chem. Phys. 25, 31726–31740. https://doi.org/10.1039/d3cp04332k.
Usmani, Z., Sharma, Minaxi, Gaffey, J., Sharma, Monika, Dewhurst, R.J., Moreau, B., Newbold, J., Clark, W., Thakur, V.K., Gupta, V.K., 2022. Valorization of dairy waste and by-products through microbial bioprocesses. Bioresour. Technol. 346, 126444. https://doi.org/10.1016/j.biortech.2021.126444.
Vieira, I.R.S., de Carvalho, A.P.A. de, Conte-Junior, C.A., 2022. Recent advances in biobased and biodegradable polymer nanocomposites, nanoparticles, and natural antioxidants for antibacterial and antioxidant food packaging applications. Compr. Rev. Food Sci. Food Saf. 21, 3673–3716. https://doi.org/10.1111/1541-4337.12990.
Vo, Q.V., Hoa, N.T., Flavel, M., Thong, N.M., Boulebd, H., Nam, P.C., Quang, D.T., Mechler, A., 2023. A comprehensive study of the radical scavenging activity of rosmarinic acid. J. Org. Chem. 88, 17237–17248. https://doi.org/10.1021/acs.joc.3c02093.
Wollinger, A., Perrin, É., Chahboun, J., Jeannot, V., Touraud, D., Kunz, W., 2016. Antioxidant activity of hydro distillation water residues from Rosmarinus officinalis L. leaves determined by DPPH assays. Compt. Rendus Chem. 19, 754–765. https://doi.org/10.1016/j.crci.2015.12.014.
Yaraki, M.T., Zahed Nasab, S., Zare, I., Dahri, M., Moein Sadeghi, M., Koohi, M., Tan, Y.N., 2022. Biomimetic metallic nanostructures for biomedical applications, catalysis, and beyond. Ind. Eng. Chem. Res. 61, 7547–7593. https://doi.org/10.1021/acs.iecr.2c00285.
Zhang, H., Du, W., Peralta-Videa, J.R., Gardea-Torresdey, J.L., White, J.C., Keller, A., Guo, H., Ji, R., Zhao, L., 2018. Metabolomics reveals how cucumber (cucumis sativus) reprograms metabolites to cope with silver ions and silver nanoparticle-induced oxidative stress. Environ. Sci. Technol. 52, 8016–8026. https://doi.org/10.1021/acs.est.8b02440.
Zhang, J., Wang, F., Yalamarty, S.S.K., Filipczak, N., Jin, Y., Li, X., 2022. Nano silver-induced toxicity and associated mechanisms. Int. J. Nanomed. 17, 1851–1864.

https://doi.org/10.2147/IJN.S355131.
Zhang, L., Zhang, M., Mujumdar, A.S., Yu, D., Wang, H., 2023. Potential nano bacteriostatic agents to be used in meat-based foods processing and storage: a critical review. Trends Food Sci. Technol. 131, 77–90. https://doi.org/10.1016/j.tifs.2022.11.023.
Ziani, I., Bouakline, H., Yahyaoui, M.I., Belbachir, Y., Fauconnier, M.L., Asehraou, A., Tahani, A., Talhaoui, A., El Bachiri, A., 2023. The effect of ethanol/water concentration on phenolic composition, antioxidant, and antimicrobial activities of Rosmarinus tournefortii de Noé hydrodistillation solid residues. J. Food Meas. Char. 17, 1602–1615. https://doi.org/10.1007/s11694-022-01722-6.